ANL-7266

ANL-7266

6/13

Argonne National Laboratory

HYDROGEN EMBRITTLEMENT IN IRRADIATED STEELS

by

A. D. Rossin

DISCLAIMER

Printed in the United States of America
Available from
Clearinghouse for Federal Scientific and Technical Information
National Bureau of Standards, U. S. Department of Commerce
Springfield, Virginia 22151
Price: Printed Copy $3.00; Microfiche $0.65

ANL-7266
Metals, Ceramics, and
Materials (TID-4500)
AEC Research and
Development Report

ARGONNE NATIONAL LABORATORY
9700 South Cass Avenue
Argonne, Illinois 60439

HYDROGEN EMBRITTLEMENT IN IRRADIATED STEELS

by

A. D. Rossin

Metallurgy Division
Metallurgy Program 6.10.17

February 1967

THIS PAGE
WAS INTENTIONALLY
LEFT BLANK

TABLE OF CONTENTS

TABLE OF CONTENTS

LIST OF FIGURES

LIST OF FIGURES

LIST OF FIGURES

LIST OF TABLES

HYDROGEN EMBRITTLEMENT IN IRRADIATED STEELS

By

A. D. Rossin

ABSTRACT

Hydrogen-charging conditions that completely embrittle Type 4340 high-strength steel have a negligible effect on 212-B pressure-vessel steel in tensile and delayed-failure tests. Much higher hydrogen charges reduce the notch-tensile strength slightly. Delayed failure is observed only at stresses above 90% of the notch-tensile strength of the hydrogenated 212-B. Tests on 212-B that had been irradiated to give a 35% increase in strength and an NDT temperature shift of 94°C showed the same relationship between delayed-failure limits and notch-tensile strength.

Catastrophic embrittlement due to hydrogen (like delayed failures at 25 to 50% of the notch-tensile strength in Type 4340 steel) was not observed in 212-B, even for irradiated material that had been charged to produce high hydrogen contents. Therefore, catastrophic hydrogen embrittlement of a well-designed nuclear-reactor pressure vessel is not believed credible.

The notch-tensile strength of Type 4340 steel was reduced by irradiation, although the tensile strength increased. Catastrophic delayed failure still occurred, but with the sensitivity to hydrogen slightly reduced.

I. INTRODUCTION

The phenomenon of hydrogen embrittlement in high-strength steels is well documented. It is characterized by sudden catastrophic brittle failure under sustained loads that produce stresses as low as one-fourth or one-half the tensile strength of the material.

Tough, ductile steels, of the kind used for nuclear-reactor pressure vessels, have much lower tensile strengths, and such behavior due to hydrogen has not generally been observed in them. Neutron irradiation hardens

these steels, raises their yield and tensile strengths, and makes them brittle at room temperature. The primary purpose of this investigation is to determine whether irradiated pressure-vessel steels could become susceptible to hydrogen embrittlement. The possibility of such failure would have serious reactor-safety implications.

Irradiation also causes a loss of strength in ultrahigh-strength quenched and tempered steels. A secondary part of this investigation is to see if the irradiated structure remains susceptible to catastrophic failure due to hydrogen.

Finally, it is desired to see if the behavior observed is consistent with the currently accepted theories on the mechanisms responsible for radiation hardening and hydrogen embrittlement.

II. BACKGROUND

A. Hydrogen in Steel

Delayed brittle failure of steel results from a combination of factors: stress, stress state, hydrogen concentration, the type of steel, and its strength. Other parameters play their parts as well in determining just how a specimen or structure will behave. Many investigations have been made of the influence of individual factors. In addition to the many original papers in the literature, some of which will be referred to below, four extensive reviews furnish valuable background information on the subject.[1-4]

Hydrogen embrittlement is a quantitative phenomenon. That is, the proper combination of the various parameters results in loss of strength, and although the effect of one can be reproducibly studied by controlling certain variables, a generalized parametric picture is not available, and would probably be too complex for purposes of design or evaluation. However, a phenomenological picture can be drawn from the experimental results available.

Hydrogen embrittlement was first observed in high-strength steels. Many investigations have since shown that the higher the strength level, the sooner a specimen will fail for a given load, or the lower will be the limiting critical stress level (lower critical stress) below which no failures are observed. A notch or other stress-raiser increases the susceptibility and localizes the point of failure.

Failure behavior depends directly on the hydrogen content of the steel, although not on the means for its entry. If the hydrogen is removed before any permanent damage takes place, no further effect is observed. The critical hydrogen concentration may not exist originally at the failure

location. It moves there by diffusion, with the stress gradient supplying the driving force. The time period before the incubation of cracks depends on the hydrogen available and the diffusion rate (hence on the temperature). At high temperatures, hydrogen will diffuse out of the specimen; at low temperatures, the diffusion rate is so slow that a critical concentration does not develop in a reasonable period of time. If the hydrogen concentration is high enough, the strength level, as determined by the tensile test, will be reduced.

Although evidence of delayed failure has been found in other structures, the body-centered-cubic structure of ferrite, and the tetragonal structure of martensite are the most susceptible. In addition, the metal must sustain enough stress without gross plastic flow or fracture to provide the necessary stress gradient and time for diffusion of the hydrogen.

Delayed failure is best studied by means of a constant-load test of a notched tensile type specimen and measurement of time to rupture. This provides a reproducible geometry giving a favorable stress distribution for delayed failure. Hydrogen can be charged electrolytically either before or during stressing, or it can be driven in by holding the specimen at elevated temperature in high-pressure hydrogen and then quenching to room temperature.

The results of tests of this type and others have led to the following picture for the mechanism responsible for delayed failure:

> The stress concentration caused by the notch allows hydrogen to build up in a localized region by diffusion. A critical concentration of hydrogen and stress leads to initiation of a crack. The time required is referred to as the incubation period.
>
> The crack allows the stress distribution to change, and the hydrogen builds up at a new location in the remaining metal. The crack propagates, and the process repeats itself until the stress on the remaining cross section of metal exceeds the fracture strength, and the specimen fails.

The remaining link in the theory is the mechanism by which hydrogen weakens the metal. There are differing schools of thought on the subject, and they hinge on the state of the hydrogen. Troiano's picture[4] calls for the hydrogen atoms or ions to occupy interstitial lattice sites. The presence of the hydrogen decreases the interatomic forces that hold the iron lattice together. The alternative theory takes various forms depending on the investigator, but requires the hydrogen to move to the surfaces of internal voids or microcracks where it takes the molecular form and accumulates. Pockets of gas of very high pressure could thus be created that tend to exert forces increasing the effective stress in the material. The gas

molecules could also adsorb to the internal surfaces of the microvoid tip and cause it to grow. In either case, the ability of the material to support stress is reduced.

The paragraphs that follow will note some of the experimental evidence that describes the behavior of hydrogenated steel. This experience provides a frame of reference on which to analyze the results to be presented.

1. Strength Level

Despite the difficulty of controlling all other experimental variables, there is clear evidence that a high strength level increases the susceptibility of the steel to hydrogen embrittlement. The strength of Type 4340 steel can be controlled by the tempering temperature; hence a family of strength levels can be obtained for one material. Frohmberg, Barnett, and Troiano[5] showed that over a range of 25% in tensile strength, the incubation period tended to be slightly shorter, and the charged notch-tensile strength suffered more for the stronger steels. Slaughter et al.,[6] show the same trend in two steels during continuous charging.

In order for preferential diffusion to take place, the metal must be strong enough to sustain enough stress to provide the driving force. Plastic flow relaxes the stress field, and gross yielding ends the test before the critical concentrations can build up. For a given load, the material with the higher strength is less likely to suffer any plastic flow, even on a microscopic level. Also, since the strains of importance are elastic, the shape of the strained lattice cell should influence the diffusion. The amount of transverse contraction of a lattice cell will depend on the strength level of the material and the multiaxial stress distribution caused by the notch. Perhaps the most effective geometry for enhancing diffusion is the lattice cell that is expanded most uniformly in all three directions. Hydrogen should accumulate preferentially in such stressed cells.

2. Notch Acuity

Hydrogen embrittlement is observed in unnotched specimens, but the presence of a notch increases the susceptibility by an enormous amount. For experimental work, tests of notched specimens give much more reproducible results. The notch causes a multiaxial stress distribution near its root. The sharper the notch, the more pronounced the triaxiality, hence the greater the driving force for preferential diffusion. Johnson, Morlet, and Troiano[7] used specimens with notch-root radii from 0.25 to 0.001 in., and this dependence is clearly shown.

3. Temperature

Diffusion at room temperature is necessary for delayed failure. Even at room temperature, some hydrogen diffuses out of the metal. This

gives rise to a dependence on aging time, the time from the end of charging until testing.[5,8,9] At higher temperatures, the diffusion rate is higher; hence, baking can be considered accelerated aging. Johnson et al.,[10] used different baking times to adjust hydrogen content, and Steigerwald et al.,[11] used delayed-failure data to determine an activation energy for diffusion. Baking at 150°C can outgas the specimens used in this study in a day, and this temperature is used for vacuum extraction.

Testing for delayed failure at elevated temperatures would result in outgassing. On the other hand, at very low temperatures, diffusion is so slow that the critical distribution does not build up at all. Charged specimens normally susceptible at room temperature can be loaded at low temperatures with no failure. On the return of the specimens to room temperature, typical delayed-failure behavior is observed.[12]

4. Hydrogen Content

The critical concentration of hydrogen that causes failure under a given stress condition is not known. Hydrogen diffuses to the point of failure and is released when the material ruptures, making it impossible to determine just how much was present. However, the total amount of hydrogen in the specimen can be determined. Of course, the higher the average hydrogen content, the shorter the diffusion time needed to build up the required concentration for failure.

The hydrogen content can be controlled experimentally by adjusting the charging conditions (or pressure, etc., if other hydrogenation techniques are used). There is probably a saturation level for hydrogen content, since many parametric studies indicate blistering at very extreme charging conditions.[13] A linear reciprocity probably exists between charging current and time at low concentrations, but it certainly becomes nonlinear at higher levels and ultimately reaches saturation conditions. Elsea[14] suggests an exponential dependence on current density and Rakzinski[15] a square root in the intermediate range.

The distribution of hydrogen in a test piece is very nonuniform after electrolytic charging, with the hydrogen near the surface. Diffusion tends to average out the concentration (if done free from stress), and this process can be speeded up by raising the temperature. Although this results in some outgassing, it can aid in making results more reproducible. The effect of subsequent aging at room temperature is rendered much less important. The escape of hydrogen from the surface can be greatly retarded by plating.[16,17] Cadmium is the most effective plate and is used in these experiments. It does not stop outgassing, but it slows the escape rate enough to permit valid stress-rupture experiments. Early work[5] examined

the delayed-failure characteristics as a function of aging time. If cadmium-plated and baked specimens are used, delayed failure can be studied as a function of stress, charging conditions, etc., without significant effects due to aging.

Much work on the effect of hydrogen in steel has been done by using methods other than electrolytic precharging. At BMI, specimens are stressed during electrolytic charging in aqueous solution.[8] At ORNL, specimens were tested in hydrogen under pressure.[18] Many investigations employed soaking in hydrogen under pressure at elevated temperatures and then quenching to retain the hydrogen. These various experiments indicate that the critical parameter is still the hydrogen content itself, regardless of the method by which it is introduced.

Small concentrations of impurities in steel are customarily reported in parts per million by weight (ppm). This is also the custom with hydrogen, but one must recall that the ratio of atomic weights is 56 to 1. Thus 1 ppm represents 56 atoms of hydrogen per million of iron. If this concentration were evolved at atmospheric pressure, it would occupy 1.11 cc per 100 grams of steel.

Considerable work on hydrogen embrittlement has been done with quenched and tempered 4340, a high-strength steel. Catastrophic hydrogen embrittlement results with concentrations of just a few parts per million. One ppm seems to be enough to cause delayed failure in 4340 tempered to 270,000 psi.[8] On the other hand, the effect of hydrogen in lower-strength bainitic and pearlitic steels was studied by Cain and Troiano.[19] They chose to charge at 200 mA/in.^{2} for 2 hr, as compared to the 20 mA/in.^{2} for 5 min that embrittled 4340. The resulting hydrogen content of the specimens was undoubtedly far less than the direct proportionality predicted by the product of the charging current and time. Delayed failure was clearly demonstrated. However, because of the low strength level, even with these charging techniques, the lower critical stress was only 30% below the original notch-tensile strength.

5. Strain Rate

In tensile testing of hydrogenated specimens, some strength loss is generally observed.[20] After the initial strain on loading in a stress-rupture test, there is practically no strain rate; diffusion has time to take place. Diffusion cannot keep up with the strain in a typical tensile test, so the observed loss in strength must be attributed to the hydrogen that is already present. Thus small differences in the loading rate in tensile testing should not have much effect on the measured tensile strength of hydrogenated steel. On the other hand, the observed loss of tensile strength should depend on the initial hydrogen content.

6. Microstructure

The most significant parameter affecting hydrogen embrittlement characteristics is the strength level of the steel. It is difficult to generalize from the literature about the relative roles of composition and microstructure, except to point out the way in which they affect strength level and crystal structure. Tempered martensite and bainite structures with the same strength levels performed in substantially the same manner,[5] although the martensite was termed slightly more susceptible, perhaps because of higher residual stresses. Cain and Troiano's work[19] indicated more susceptibility for normalized steel than for bainite of the same strength level.

Although there is some evidence of hydrogen embrittlement in austenite,[21] the conditions required are very severe. In general, because of higher solubility of hydrogen, the face-centered-cubic phase is much more tolerant of hydrogen, and therefore not subject to such embrittlement. Alloying elements that tend to promote the formation of austenite tend, as a result, to reduce the likelihood of hydrogen embrittlement.

B. Radiation Embrittlement

There is a vast literature on the effect of neutron irradiation on the mechanical properties of steel. In general, sufficient exposure to fast neutrons causes hardening, raises the yield and tensile strengths, and raises the brittle-ductile transition temperature. Although similar behavior is observed in stainless steels, particularly in loss of ductility, the required neutron exposure is one to two orders of magnitude greater.

The mechanism is as follows: the fast neutron, with energy in the range of a million electron volts, strikes an iron atom. Some of its energy is transferred to this primary atom. It recoils and knocks many other atoms out of their lattice sites. Since it only takes 25 eV or less to displace an iron atom, and on the average the neutron transfers about 3% of its energy to the primary struck atom, there is enough energy available to displace many hundreds of atoms per neutron-iron interaction. These atoms end up in interstitial positions; they form clusters and tiny regions rich in vacancies or extra atoms. These all impede the motion of dislocations, reducing the ability of the metal to flow, and producing the changes in mechanical properties mentioned above.

1. Pressure-vessel Steels

Most pressure vessels for boiling-water or pressurized-water reactors are made of carbon steel clad with stainless steel to prevent corrosion. To assure the safety of the reactor, the vessel steel must remain

tough and ductile, so that a crack cannot propagate. Therefore, the embrittling effect of neutron irradiation has been studied extensively, in particular the loss in ductility and the rise in the transition temperature. Conservative design practice does not permit taking advantage of the increase in yield strength during the life of the structure.

The steel chosen for this investigation, A212-B, has been used in a number of reactor vessels: EBWR, some military reactors, and some large central-station power reactors. Other experimenters have shown that the yield stress rises with neutron exposure; increases as great as 60 to 100% have been reported at very high exposures.[22-24]

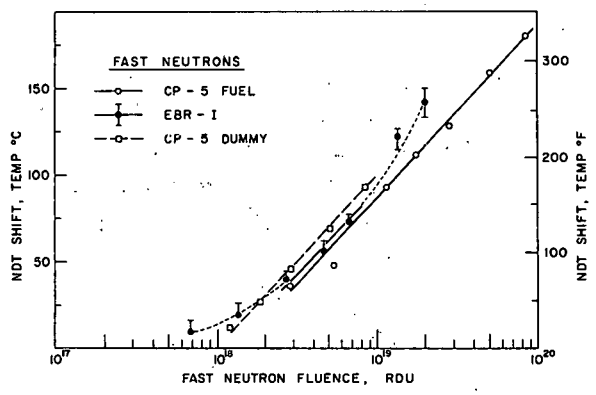

106-8823 Rev. 1

Fig. 1. Shift in Nil-ductility Transition Temperature vs Fast-neutron Fluence

The rise in transition temperature suggests a logarithmic dependency, as Fig. 1 shows.[25,26] The neutron exposure is given in RDU, (radiation damage unit), a unit developed by the author,[27] and its use is demonstrated in this report. Each RDU is equivalent to one fission neutron; 69% of all fission neutrons have energies greater than 1 MeV. Design lives for power-reactor vessels are set in the range of 10^{18} RDU, unless the vessel is to be kept above the calculated nil-ductility transition temperature by a specified margin whenever it is pressurized. Figure 1 is based on impact-test data. Since no impact-test specimens are used in this study, the RDU exposure is to be determined and the change in transition temperature of the 212-B will be estimated from this plot.

2. High-strength Steel

Very little data exist on the effect of high neutron exposure on high-strength steels. There has been a reticence to use these steels in reactors for fear that radiation will affect the quenched structure that gives the material its strength. Bad experience with cracking in 17-4PH steel hardened to a high strength practically eliminated interest in these steels for critical reactor parts.

C. Hydrogen in Irradiated Steel

Most of the power reactors now operating in the United States, or currently under design, are pressurized- or boiling-water cooled and moderated. The safety of the entire reactor system depends on the integrity of the reactor pressure vessel. Under no circumstances could a brittle

material be counted on to do the job required of these vessels, nor could one permit the use of a material that could be subject to catastrophic failure at low stress levels because of hydrogen embrittlement. If the stainless steel cladding should fail, water could come in intimate contact with the steel vessel. Thus, a source of hydrogen is available, and the danger of hydrogen embrittlement must be considered.

During 1965, two instances were discovered of breaches in stainless steel cladding material on the inner walls of reactor vessels. The EBWR at Argonne, a boiling-water reactor, has a 212-B pressure vessel with a quarter-inch-thick stainless steel liner. Cracks were found in this cladding, and were attributed to thermal stresses developed in the cladding due to the roll-spot welding technique used to fasten the stainless steel to the carbon steel.[28] The cracks did not penetrate the vessel wall itself. The Yankee pressurized-water atomic power plant suffered erosion of its stainless steel cladding where some small steel surveillance specimens, which had broken loose from their mountings, had rubbed against the wall.[29] Some of the 302-B carbon steel vessel wall had been exposed to the coolant water.

In each of these cases, reasons were present that ruled out any significant danger from hydrogen embrittlement. The operating temperature is high enough (~260°C) to outgas hydrogen quite readily, so even if a constant source is available the equilibrium concentration must remain low. For the Yankee plant, the maximum concentration predicted during operation from all possible hydrogen sources is 0.32 ppm at the inner surface, decreasing to the outer surface of the vessel wall.[29]

Since the diffusion rate is so much lower at room temperature, the maximum equilibrium concentration of hydrogen after a prolonged shutdown was estimated at 1.2 ppm. Granted that one might take issue with several of the simplifying assumptions used in these estimates, they furnish a place to start for evaluation of potential hazards.

Broomfield[30] tested a chromium-molybdenum pressure-vessel steel in tension between room temperature and 250°C. Hydrogen was introduced at 250°C under 1750 atm pressure, followed by cooling in hydrogen to the test temperature. A hydrogen concentration for a room-temperature test was estimated at about 1.3 ppm.

Broomfield's tensile tests showed little effect of hydrogen on 0.5% proof stress or tensile strength. However, hydrogen definitely reduced the elongation, the reduction of area, and the breaking stress, the effect being greatest at the lower temperatures. There was little difference between irradiated and control material in these tests.

Two delayed-failure tests were attempted. However, the two specimens were loaded for 30 days at about the yield stress with no failures, then outgassed for 6 hr at 250°C, and finally tensile-tested in argon gas. The tensile strength was higher than for the controls, but the difference is not attributable to hydrogen. This effect is typical of tensile tests of steel that has been subjected to previous loading.

Since the main effect of irradiation is to embrittle carbon steel, it is possible that irradiation could increase the susceptibility of the material to delayed failure due to hydrogen. The influence on delayed failure of increased yield stress might well be the same if the hardening is caused by irradiation, rather than by different heat treatments. By prevention of the onset of plastic flow at a high enough stress level, time is made available to allow hydrogen diffusion, which can result in premature failure under sustained load.

The effect of the tremendous number of point defects, clusters, and interstitials caused by the irradiation on the diffusion of hydrogen is not known. These imperfections might act as traps to prevent further diffusion. On the other hand, such regions might be ideal sites for internal cracks to nucleate. It seems reasonable to predict that the susceptibility to delayed failure should increase on irradiation because of the increase in strength, with the changes in internal structure perhaps exerting a secondary influence on the material behavior.

III. APPROACH

A. General

The problem to be considered is that of hydrogen embrittlement in irradiated steel. Two highly different aspects are examined by studying the behavior of two very different steels. First, a high-strength steel was irradiated and then hydrogenated and tested in the manner in which it had previously suffered catastrophic embrittlement. Quenched and tempered 4340 was chosen, since ample documentation of its behavior is found in the literature. Thus, unirradiated 4340 could serve as a control material, although it was not proposed to reproduce published data. By a comparison of its performance with data found in the literature, a check could be obtained on the hydrogenation procedure with a relatively small number of tests.

It is also of interest to find out what neutron irradiation does to the performance of the hard, strong, quenched and tempered structure of the 4340. (This steel has not been used for reactor internal components, although other heat-treated steels have.) Would the irradiation raise its extremely high strength even more, or would it reduce it substantially? How would hydrogen then affect its behavior? Hence, tests on irradiated 4340 were included in the program.

The other phase of the work, and the one bearing on significant questions of reactor safety, deals with the possibility that a tough, dependable, familiar pressure-vessel steel might become susceptible to hydrogen embrittlement after being exposed to neutron irradiation. Steel A212-B, the vessel material for Argonne's Experimental Boiling Water Reactor and of a number of other pressurized- and boiling-water reactors, was chosen. In addition to the obvious interest because of its current use in reactors, this choice offered the advantage of an available supply of completely documented test plates, obtained and stored under the AEC program on Radiation Effects in Reactor Structural Materials.

The literature contained no evidence that hydrogen embrittlement was a problem in 212-B. However, the possibility discussed above, of a tough steel becoming hard and brittle due to neutron bombardment, and then being susceptible to catastrophic delayed failure, could not be ruled out.

Low-carbon steels can be embrittled by hydrogen, but only under special conditions. Only relatively higher-strength steels can be embrittled, and hydrogen concentrations a number of times as high as those required to embrittle 4340 are required. Such conditions were sought by increasing both the charging time and the charging current by sizable factors.

Samples of 212-B were to be irradiated to an exposure large enough to raise its ductile-brittle transition temperature well above room temperature and to cause a substantial increase in its yield and tensile strength. This material would then be hydrogenated and tested in the manner that revealed catastrophic delayed failure in 4340. If no embrittlement could be detected, even under extremely severe hydrogenation, the danger of catastrophic delayed brittle failure in reactor pressure vessels of 212-B due to hydrogen embrittlement could be confidently eliminated from consideration. On the other hand, if catastrophic delayed failure were observed, further experimentation would be required to determine the critical conditions of hydrogen concentration and stress sufficient to produce embrittlement.

Susceptibility to hydrogen embrittlement is determined by stress-rupture tests on notch-tensile specimens. Even without hydrogen, steel will fail under load if the stress level is only slightly below the tensile strength. Catastrophic embrittlement implies a significant lowering of the ratio of failure load in stress-rupture testing to the notch-tensile strength. Charged 4340 is known to fail at less than 25% of the notch-tensile strength, well below the yield stress. It seems prudent to define the delayed failure range for 212-B as catastrophic if it reaches down to the tensile strength or the notch yield strength of the material, and certainly if the lower critical stress is below the yield stress.

Thus, this investigation involves the following:

1. Setting up facilities suitable for use with radioactive specimens for hydrogenation of the two steels.

2. Providing tensile and stress-rupture machines for testing controls and irradiated specimens.

3. Irradiating in the CP-5 reactor a capsule containing both materials to an exposure high enough to neutron-embrittle the pressure-vessel steel.

4. Proving that the hydrogenation procedure used produced catastrophic failure in 4340.

5. Testing the irradiated 4340 to see if its behavior differs with and without hydrogen.

6. Determining delayed-failure characteristics of 212-B.

7. Performing sufficient tests to prove whether the irradiated pressure-vessel steel would or would not become susceptible to catastrophic hydrogen embrittlement.

8. Constructing equipment to attempt to measure the hydrogen concentration in charged specimens.

B. Terminology

The following definitions apply throughout this report:

Tensile Strength (TS): Maximum load in the tensile test of an unnotched specimen, divided by the initial minimum cross-sectional area.

Notch-tensile Strength (NTS): Maximum load in the tensile test of a notched specimen, divided by the original cross-sectional area at the notch.

Yield Stress (YS): The stress level at which the strain breaks away from the straight elastic stress-strain line. This term will be used with tensile tests of 212-B.

0.2% Offset Yield Stress (0.2% OYS): The stress level, based on load divided by original cross-sectional area, at which the strain is 0.2% greater than that given by extrapolating the initial straight elastic stress-strain line. This term will be used with the 4340 tensile data.

Notched Yield Strength (NYS): The stress level, based on load divided by original cross-sectional area of a notched tensile specimen, at which the strain breaks away from the straight elastic stress-strain line.

Lower Critical Stress (LCS): The stress level below which a notch-tensile specimen does not fail in 100 hr under constant load.

Nil-ductility Transition (NDT): An empirically refined characteristic temperature. The temperature below which a material shows no ductility in a standardized impact test is known as the nil-ductility transition (NDT) temperature.

IV. PROCEDURE

A. Materials

Details of the compositions and properties of the materials used are presented in Appendix A.

The 4340 was obtained from Osco Steel Co. in the form of 5/8-in.-diam round bar stock. The composition is given in Table A-I. Specimens were machined to size, including the rough notch. The specimens were then heat-treated to a Rockwell C hardness of 49 to 51 by the procedure in Appendix A. Then the fine notch was cut in the hardened material, and the final surface finishing was done on the shaped specimens.

The 212-B was obtained from the stockpile of materials of interest to the USAEC program on Radiation Effects in Reactor Structural Materials at the Battelle Pacific Northwest Laboratory. Complete documentation on the 4-in. cross-rolled plate is given in Table A-II, as furnished by the supplier of the material and reported in BNWL-CC-236.[31] The plate was sectioned and the specimens machined from the quarter-thickness sections. Specimens were cut parallel to the final rolling direction.

B. Specimens

Two specimen shapes are employed in this work. They have been used successfully in previous work at Case Institute of Technology and are referred to extensively in the literature.[20] The buttonhead design proved easily adaptable to remote handling, as was required for the irradiated specimens.

The notch-tensile specimen has been designated Type J at Case. Its dimensions are shown in Fig. 2. In the machining process, a rough notch was cut to a root diameter of 0.215 in. and in a separate operation a fine notch was cut to a root diameter of 0.212 in. (0.538 cm). Each specimen was shadowgraphed, and the actual diameter and root radius determined. The fine notch-root radius is specified to be 0.001 in., and most notches appeared to meet this criterion, though in no case was a specimen used that had a notch-root radius greater than 0.002 in. It was decided that specimens would be acceptable as long as the notch diameter was within ± 0.002 in. of the nominal 0.212 in., since the difference in cross-sectional area would result in misstating stress values by no more than 2%, which is of the order of the expected statistical variation of tensile-test results. More important, stress-rupture tests of hydrogenated specimens that fail soon after loading, or hold for more than 100 hr are not compromised by this variation.

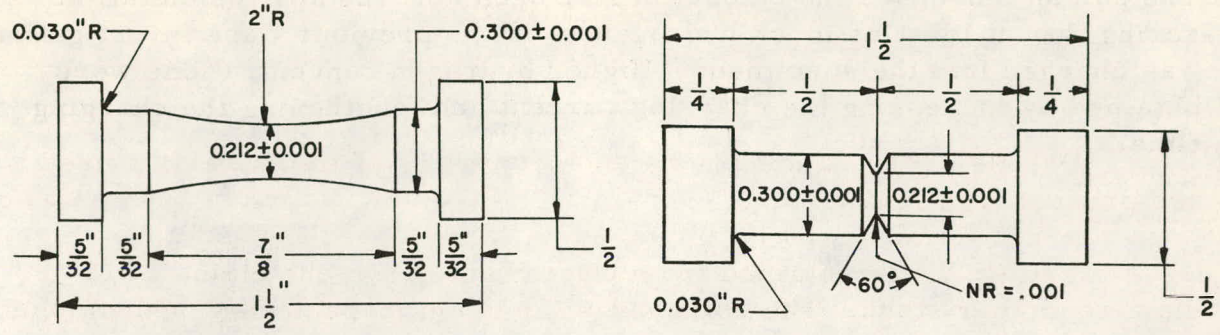

106-8824

Shaped Tensile Specimen

Notched Tensile Specimen

Fig. 2. Test-specimen Design; Shaped (E) Type, Notched (J) Type

The shaped tensile specimens (Type E) were specified to be polished so as to have no radial scratches that might lead to unexpected stress raisers in the gage section. The minimum diameter of each specimen was within 1/2% of the specified 0.212-in. diam.

Identification markings were stamped on the ends of the specimens. For the 212-B specimens, a single digit served three specimens, thus, 4, 4, 4. A group of three like this were placed in one tier in the irradiation capsule, so all three received the same neutron exposure. Since the 4340 material was too hard for good stamping of numbers, hardness indents were used to identify the specimens. The number of indents on each end was noted; thus . ∴ has one indent on one end and three on the other. These simple markings proved easy to read through the thick windows of the hot cell. For reporting data, the tier number was inserted; thus · 13 ∴ was irradiated in tier 13.

Unirradiated specimens were usually not marked in this way. They were placed in transparent plastic envelopes having a designation written on the envelope. By keeping the specimen in or with the envelope at all times, identification was easily maintained, and handling minimized.

C. Hydrogenation

The equipment for charging and plating of specimens was kept as simple as possible for adaptation to remote handling. The setup in the hot cell is pictured in Fig. 3.

The procedure chosen for charging the specimens with hydrogen is based on Case "Charging Condition A."[5] The electrolyte is 4% H_2SO_4 in water, and the anode a platinum screen. Condition A uses a current density of 20 mA/in^2 for 5 min. The procedure chosen uses 10 mA/in.^{2} (1.55 mA/cm^2) for 10 min, which corresponds to 25 mA for a J-type specimen. A small amount of sodium arsenate "poison" is added to the solution.

The poison increases the amount of hydrogen absorbed by the metal, assuring that at least as much hydrogen as in the previous Case investigations was charged into the specimens. Higher hydrogen concentrations were obtained by increasing the charging current and lengthening the charging time.

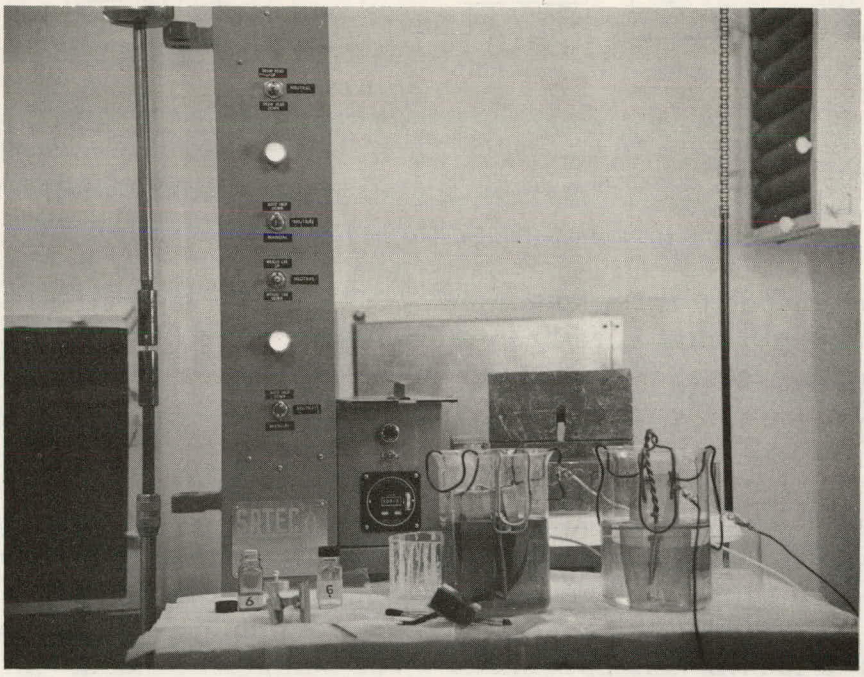

Fig. 3. Stress-Rupture Machine and Charging and Plating Equipment in E-wing Hot Cell

Johnson et al.[17] demonstrated that the rate of outgassing of hydrogen from steel can be drastically reduced at room temperature by plating the specimen with cadmium. Cadmium plating was performed in a commercial cadmium-plating bath with the addition of about a teaspoonful of organic "brightener" per liter of solution. A current density of about 130 mA/in.^{2} (330 mA for a J-type specimen) was applied for 20 min. A smooth-appearing, bright gray plate was obtained. Under a low-power binocular microscope, the plating appeared to consist of tiny globules. Occasionally bulges could be observed in the plate as it dried just after plating. Some hydrogen bursts through the plating, but the performance of the plated 4340 specimens clearly indicated that, if outgassing did take place, enough hydrogen remained in the specimens for many days to give test results identical to those obtained shortly after charging.

A short bake at a moderate temperature gives the hydrogen a chance to distribute itself more uniformly throughout the specimen, since diffusion at room temperature is slow enough to keep the concentration near the surface quite high after charging. Specimens were generally baked for 1/2 hr

at 150°C. The baking treatment was deliberately omitted in a few cases to see if any differences could be observed. Apparently the cadmium effectively eliminates the aging time as a variable, at least within a week of charging and plating.

Baking at 150°C will outgas hydrogen. As indicated in Section II, baking is used to adjust the hydrogen concentration in the specimen. Outgassing is slowed by the cadmium plate, but not prevented, and check experiments were run to verify this fact. A short bake time of 30 min was chosen although this left too much hydrogen in the 4340 to show typical delayed-failure characteristics. The tensile strengths themselves were drastically reduced. However, the idea was to look for delayed failure in the 212-B with at least enough hydrogen in it to embrittle the 4340 catastrophically. The delayed-failure behavior of the 4340 was easily verified by a spot check of previously reported behavior based on longer baking times.[10]

D. Hydrogen Analysis

A glass vacuum system was constructed to measure the amount of hydrogen that could be outgassed from a specimen. The literature concerning the measurement of hydrogen concentrations in test specimens is quite inconsistent. While this particular effort will not settle the confusion, some hydrogen concentration values were obtained with this equipment, and are reported.

The system is shown schematically in Fig. 4 and pictured in Fig. 5. A calibrated volume is shown with additional calibrating bulbs and a tap for collecting gas specimens for analysis, and a vertical McLeod gage for pressure determinations. This volume is fed through a Toepler pump, whose exit valve marks the end of the calibrated volume. A mercury diffusion pump draws the gas from the specimen, which can rest in vacuum storage at room temperature, or can be moved by a magnet into a furnace. The system was calibrated with helium.

The furnace was generally kept at 150°C because this temperature was used for baking, and because indications were that outgassing could be practically completed at this temperature in a matter of hours. Methane formation is negligible at 150°C. Numerous investigators have shown that there are two temperature ranges for hydrogen outgassing, the higher beginning above 205°C. The diffusible hydrogen, responsible for delayed-failure behavior, is supposed to outgas in the lower range; the occluded hydrogen (molecular, or otherwise trapped) can only be outgassed at higher temperatures.

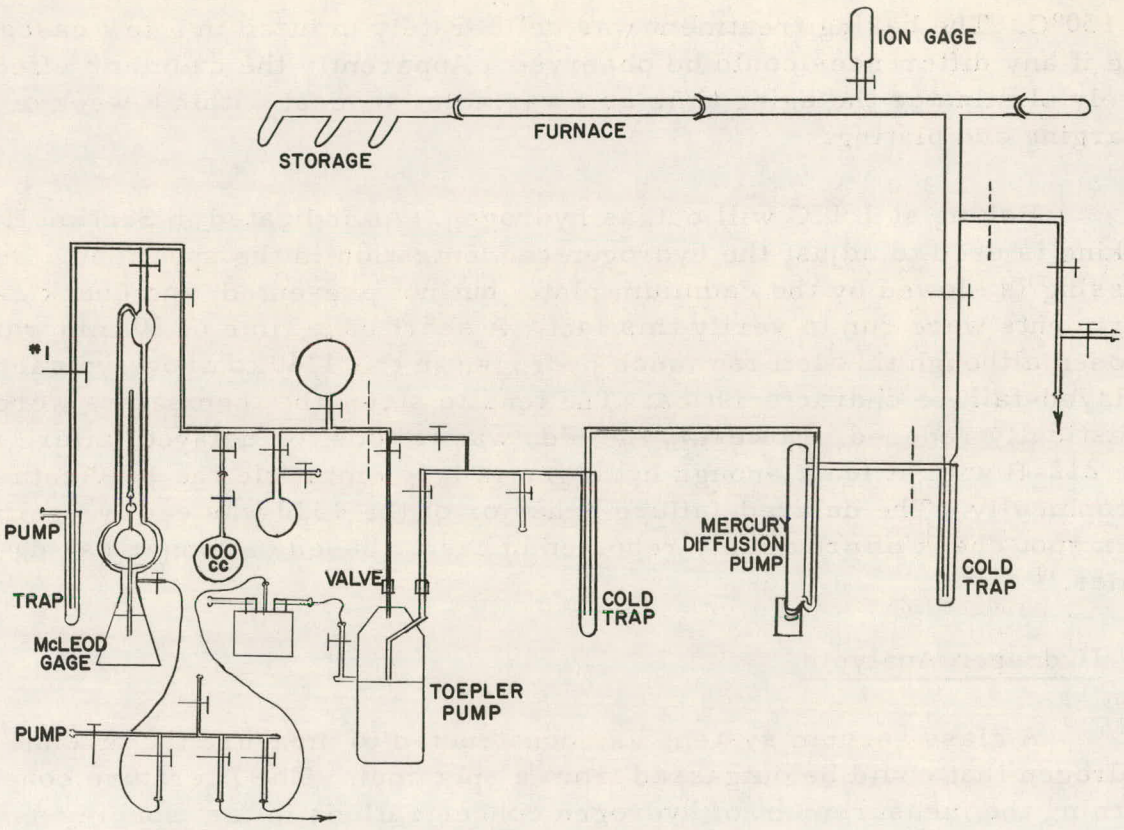

Fig. 4. Schematic Diagram of Vacuum Extraction System

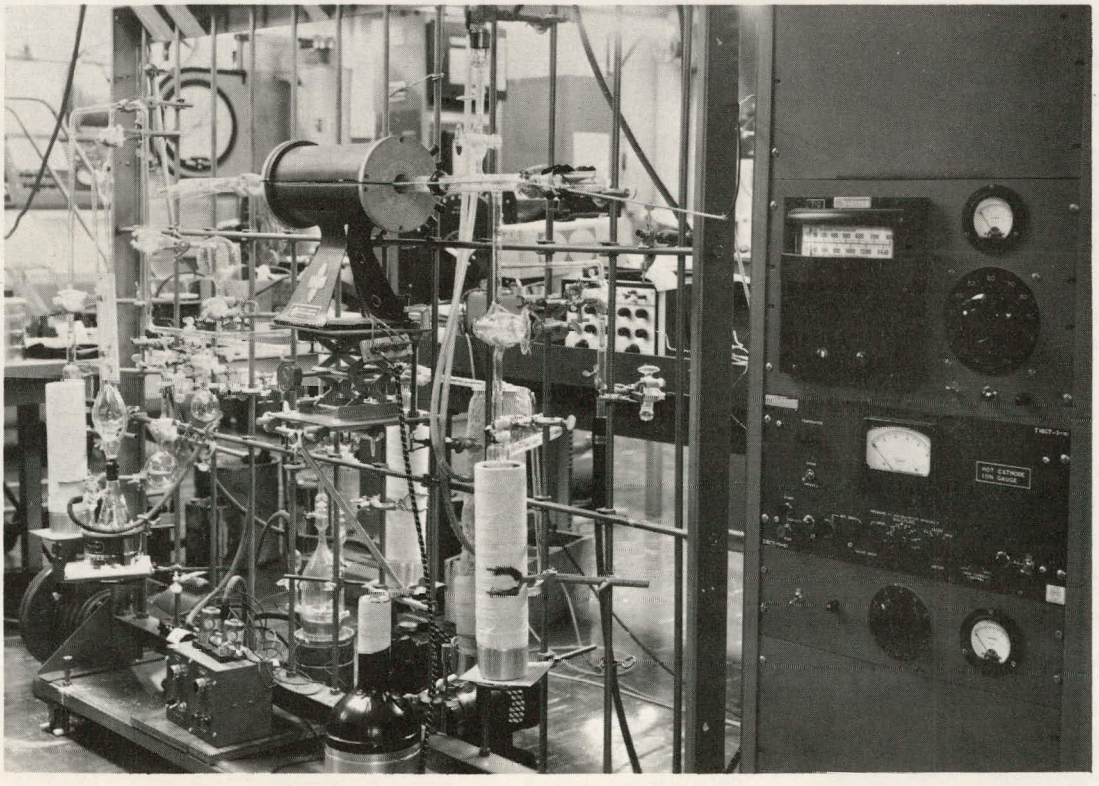

Fig. 5. Vacuum Extraction System

E. Irradiation

The steel specimens were irradiated in the Argonne National Laboratory research reactor CP-5. It was calculated that sufficient neutron exposure to make the 212-B steel brittle at room temperature could be obtained in the center of a CP-5 hollow fuel element in an irradiation of a few weeks. A 5-week irradiation was requested, but because of a change in the reactor operating schedule, only 15 days of exposure were obtained. This period proved to be sufficient for the purposes of the experiment.

The specimens were placed in a basket made of Zircaloy-3 and the basket enclosed in a double-walled, stainless steel capsule. The capsule was then filled with NaK to act as a heat-transfer bond to carry off the heat generated in the capsule and specimens from gamma radiation. Three thermocouples were included. The capsule ends were welded in place and helium leak checked. The basket, thermocouples, and capsule before assembly are pictured in Fig. 6, and the fully assembled basket is shown in Fig. 7. The thermocouple leads were brought out the top through an extension tube. A flange at the top of this tube sealed the reactor hole and provided a reference to fix the vertical position of the capsule in the irradiation thimble.

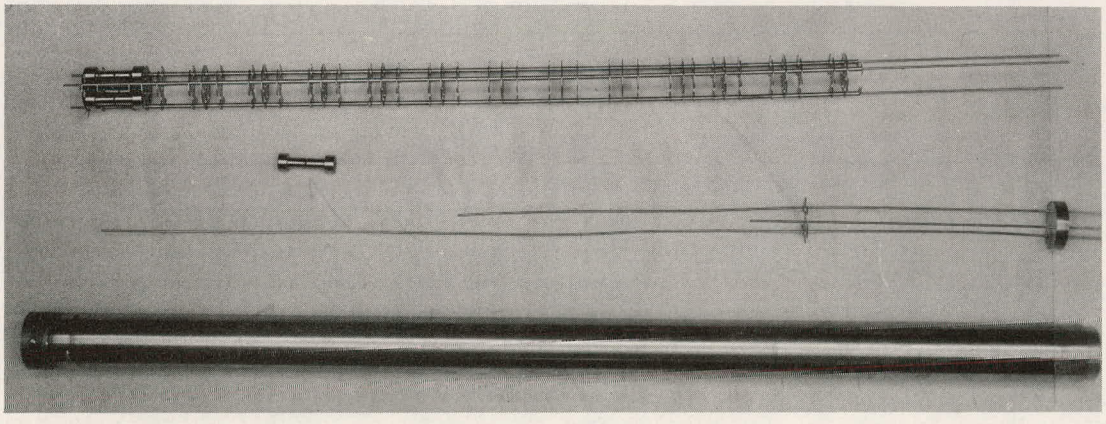

Fig. 6. Basket, Thermocouples, and Irradiation Capsule

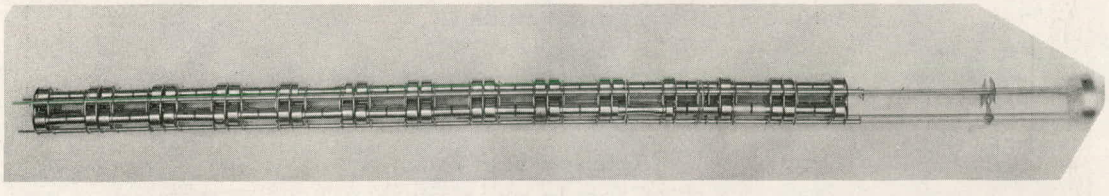

Fig. 7. Basket Completely Assembled

Table I identifies the specimens in each of the 11 tiers of three specimens each. The operating and temperature history of the capsule is given in Table II.

TABLE I. Arrangement of Specimens in Capsule

Tier No.	Distance below Top, in.	Description	Foil Wire	
			Top	Bottom
1	6.9	3 Notched 212-B	Fe, Co	Al
2	8.4	3 Notched 212-B, Thermocouple No. 1	Fe	Ni
10	10.0	3 4340 Notched Rounds	(Fe, Co, Ti, Ni)	
11	11.1	2 Notched, 1 Shaped 4340	Fe	Al
12	12.6	3 Notched 4340	Fe	Ni
3	14.2	3 Notched 212-B	Fe	Ni
4	15.8	3 Notched 212-B, Thermocouple No. 2	Fe, Co	Fe
5	17.4	3 Notched 212-B	Fe	Fe
13	18.9	2 Notched, 1 Shaped 4340	Fe	Ni
14	20.6	2 Notched, 1 Shaped 4340	Fe, Co	Fe
6	22.1	3 Notched 212-B	Fe	Fe
7	23.7	3 Notched 212-B	Fe	Ni
0	25.5	3 Notched 212-B, Thermocouple No. 3	Fe, Co	Fe

TABLE II. Irradiation History of Capsule

Date	Time	
8-10-65	1845	Capsule inserted into VT-10 of CP-5
8-10-65	2350	Capsule removed to replace flange gasket to eliminate vibration
8-11-65	1230	Reactor at power again
	1550	Temperature steady Top 73°C Middle 67°C Bottom 66°C
8-25-65	0800	Temperatures Top 75°C Middle 69°C Bottom 65°C
8-25-65	0900	Reactor shut down Capsule moved to canal
2-15-66		De-encapsulation

Integrator at Shutdown 198354160 kW/hr
at Insertion 197040710

Integrated Power = 1313450 kW/hr
= 4.728×10^6 MW-sec

Dosimetry information was obtained from irradiated metal foils. In this case, the "foils" were wires of iron, nickel, or aluminum with 0.12% cobalt. These wires were wrapped around the specimen tiers and helped to hold them firmly in place in the basket. Analysis of the activated wires and its interpretation form a separate topic and will be discussed in some detail in Section V. Some description of CP-5 and the location of the capsule are presented there and in Appendix B.

F. De-encapsulation

After the shutdown of CP-5 on August 25, 1965, the capsule was removed from the reactor, the thermocouple leads were cut off, and the capsule stored under water in the CP-5 storage canal. Since the materials in the capsule and the capsule wall were highly radioactive, no handling of the capsule was possible without high-level shielding. It was necessary to wait until testing equipment was set up and control tests completed before opening the capsule and testing the active samples.

On February 15, 1966, the capsule was removed from the canal and transferred in a 1.4-ton lead cask to Argonne's hot laboratory facility, Building 301. The extension tube was cut off, and the 27-in.-long stainless steel capsule was placed in a sealed vacuum box inside the hot cell. This box had been designed for work with irradiated plutonium samples. It has a glass front face to permit viewing of operations, and is designed to permit remote manipulators to operate in it. A view into this box, with the capsule mounted in a vertical cutoff jig, is shown in Fig. 8.

The sealed box was used so that the capsule could be opened in an oxygen-free atmosphere. This was necessary to prevent oxidation of the NaK, which had been used as a heat-transfer bond. Oxidation would probably cause sticking of the basket inside the capsule, making it difficult to remove it and the specimens, and the resulting smoke would make it impossible to see the operations in the cell. The oxygen content of the atmosphere in the box was reduced to about 1% before the cutting operation began.

The rotary jig held the capsule in a vertical position and rotated it while a cutting tool was pressed against its side. The cut removed a cap about an inch long. The thermocouple leads remained welded to this cap, and the basket could be lifted by pulling upward on the cap (see Fig. 9). A preliminary look showed the basket and specimens to be intact, and the NaK to run quickly off the specimens rather than to cling to them. The thermocouple leads were cut to remove the cap, and the stubs of the leads were used to lift the basket from the capsule and deposit it in a tray. There

it was rinsed with butyl alcohol to dissolve the residual NaK. Then it was spray-washed with APCO 140 solvent to remove the alcohol (see Fig. 10). Finally, the basket was coated with glycerine and removed from the sealed box through a lock section into an adjacent hot cell. The capsule and the remaining NaK were sent to radioactive waste disposal.

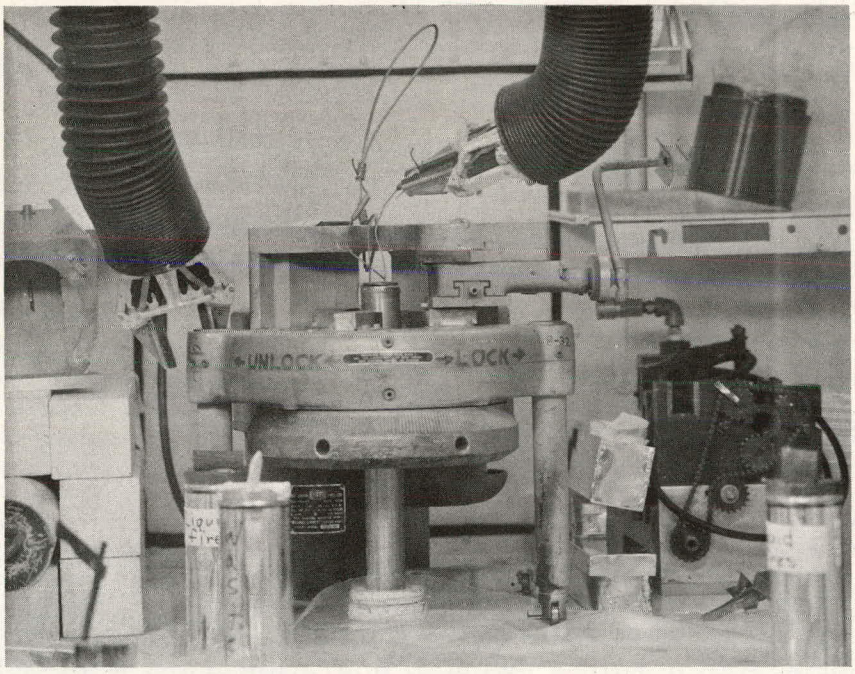

Fig. 8. In Hot Cell for Disassembly; Capsule in Jig

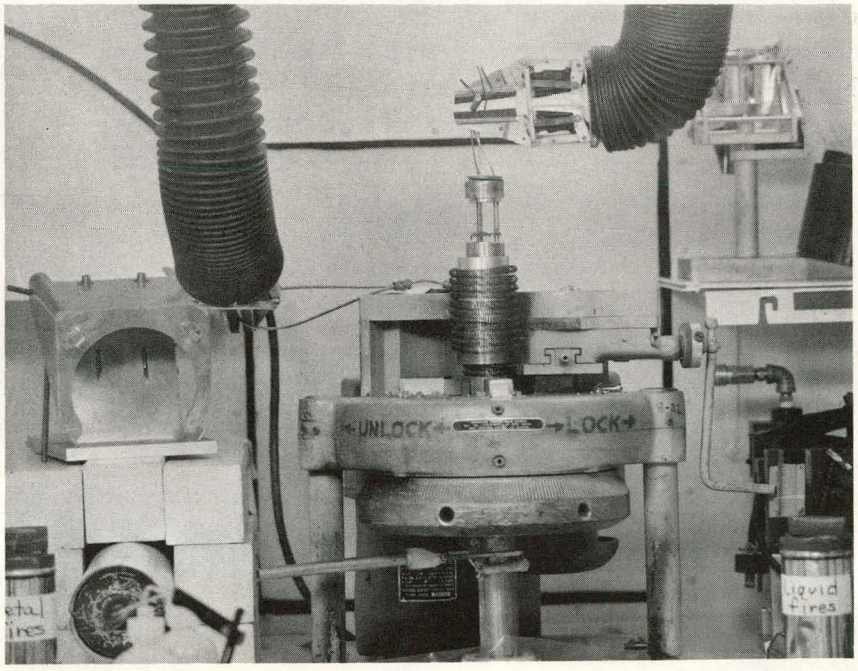

Fig. 9. Basket Being Lifted by Its Cap

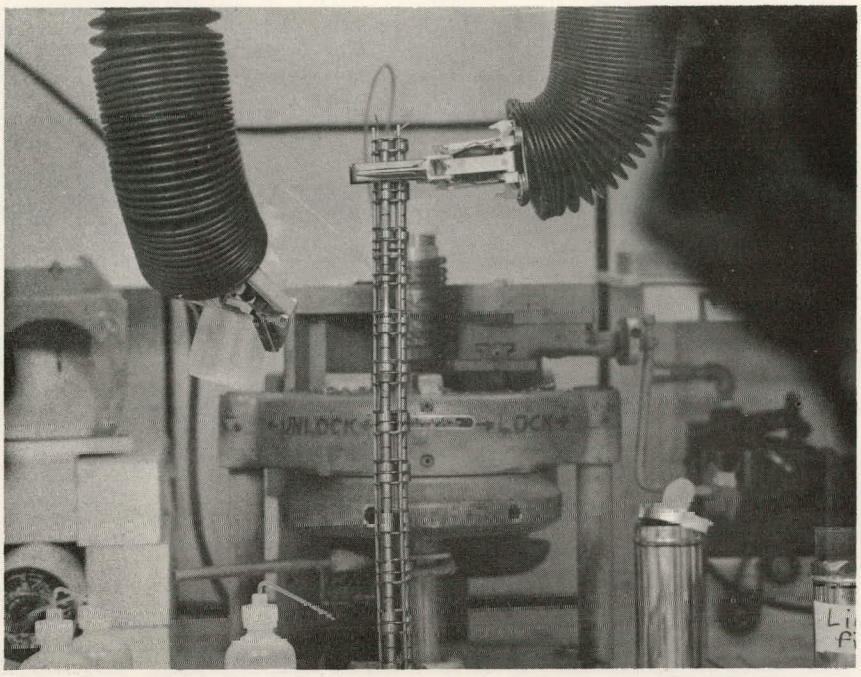

Fig. 10. Rinsing the Basket with Solvent

The use of the sealed box was not without its problems. Although it had been carefully cleaned, the box had previously been used to handle plutonium; hence it remained "suspect for alpha-particle contamination." To remove the specimens from the sealed box and handle them anywhere else in the Laboratory, extreme care had to be used, and rigid inspection requirements met.

The basket was placed in a metal tube, and the tube sealed with a gasketed cap. This assembly was removed to an adjacent hot cell where smears were taken of the glycerine coating on all the specimens. These were checked for alpha contamination. When the assembly was finally declared free of alpha contamination, it could be handled as any other radioactive metal in the regular hot cells.

Sixty bottles 1 in. square and 2 in. high with screw caps were labeled and placed in the cell with the basket. Each specimen and each foil wire, as it was removed from its place in the basket, was put into its own bottle (see Fig. 11). Those containing foil wires were put into appropriate shielded containers and shipped to the counting facility. The specimens were divided into two groups, one for immediate tensile tests, the other for hydrogen charging and subsequent tensile or stress-rupture testing.

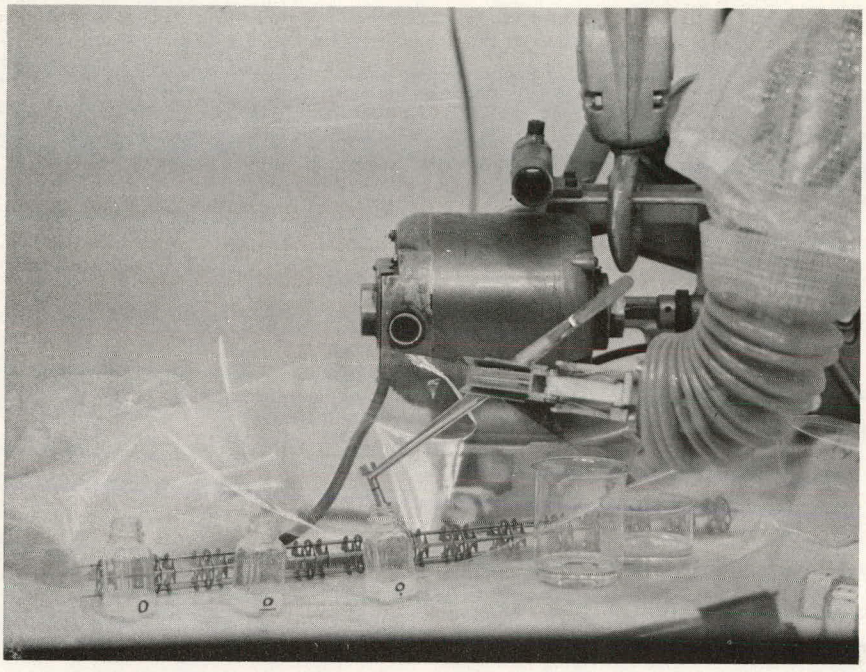

Fig. 11. Placing Specimens in Marked Bottles

G. Dosimetry

Measurement of the neutron exposure of the specimens has two purposes. The magnitude of the time-integrated neutron exposure is important because it is a condition of the experiment that the 212-B specimens be effectively embrittled by the irradiation, that is, that their ductile-brittle transition temperature be raised to well above room temperature. In addition, for future work or practical applications, the actual fluence (time-integrated neutron flux) must be known for comparison with other experimental results or design conditions.

The second aspect of the dosimetry effort is to provide a flux profile, that is, a measure of the relative fluences to the different specimens. The basket of specimens is almost 2 ft long (as long as the core of the CP-5 reactor), and the flux distribution over the length of a reactor core has the general shape of a chopped cosine, peaking near the center. It was anticipated that the difference between maximum and minimum fluence in the basket would be 15 to 20%. By exposing foils at each specimen a complete profile could be obtained with adequate statistics to be confident about its shape. Thus differences in the behavior of irradiated specimens could be analyzed in terms of differences in relative fluence.

For relative fluence measurements, the individual foil wires were supplemented by one long iron wire strung the full length of the assembly. The wire is activated by fast neutrons by the reaction $Fe^{54}(n,p)\,Mn^{54}$, with the required neutron energy above 4 Mev. Although such neutrons

are in the high-energy tail of the fission spectrum and represent a very small fraction of the total neutrons present, variations in the neutron spectrum shape over the capsule length can be ignored for relative fluence evaluation.

Activity values in disintegrations per second per milligram (dps/mg) were determined by R. J. Armani and D. M. Smith of the ANL Reactor Physics Division. Neutron exposures were then calculated according to procedures described in ANL-6826.[27]

H. Testing

Some tensile tests were performed on a Baldwin-Southwark testing machine located in the pot storage area adjacent to the hot cells. Maximum load data were obtained from tests on this machine. Yield-strength loads and failure loads were estimated by eye, using the pacing disk on the machine; hence they must be treated as approximate.

The stress-strain curves in this report were taken from Instron data. The strength of the specimens is high enough that deformations in the load train of the machine exceed those of the specimens. In the elastic range, they are about four times as great as the elongation of the specimens, but after the 212-B yields, the specimen elongation is almost equal to the crosshead movement. Elongations were measured from the separation of the grip faces.

Two SATEC stress-rupture frames were used for the studies of delayed failure (see Fig. 12). After most of the control tests were completed, one of the machines was moved into a small hot cell. The entire cell was almost filled, as shown in Fig. 3. Glassware and leads for charging and plating the specimens can also be seen. The entire front panel (2 ft of heavy concrete with its liquid-filled window) can be moved out to permit access to the cell. This was necessary to change the weights on the stress-rupture machine and to transfer specimens from casks to storage locations.

The irradiated specimens in their 1-in. square glass bottles gave off gamma radiation of about 2 R/hr intensity on contact; but at 1 meter (arm's length plus length of a pair of tongs), the activity measured about 10 to 20 mR/hr. Since a field of 7.5 mR/hr is permissible for 40 hours' exposure in a working week, handling of specimens with tongs was feasible. This had to be done many times, but the total exposure received by personnel involved during these brief periods was below permissible limits. Touching the specimens, however, was never permitted. This ability to handle the radioactive specimens was important for tensile testing, since the major problem of moving a tensile machine into a hot cell and then doing all the testing remotely was avoided.

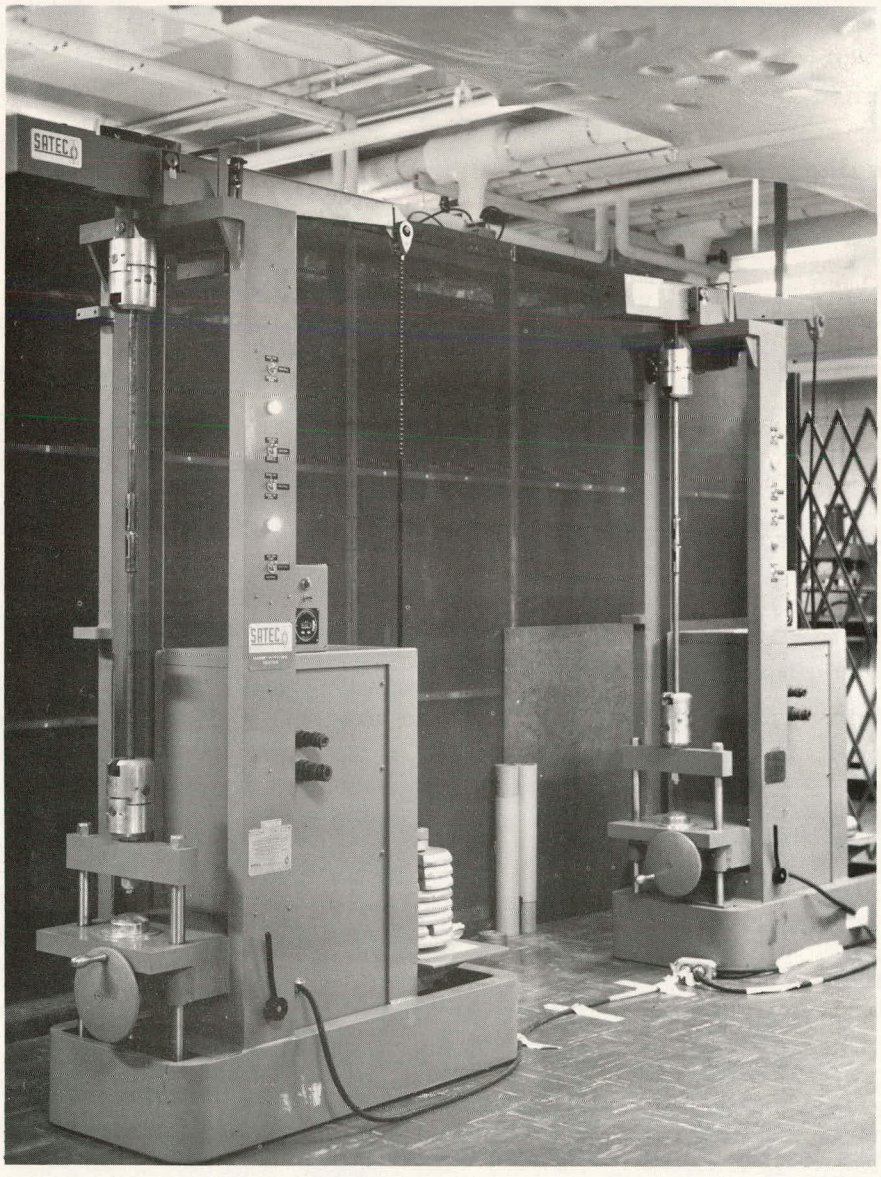

Fig. 12. Stress-Rupture Machines for Unirradiated Delayed-failure Testing

V. RESULTS

A. Hydrogen Content

The electrolytic charging technique provides a controlled method for the introduction of hydrogen. With care, it can yield reproducible results, but variables such as surface condition, contaminants in the charging solution, amount of poison present, agitation of the solution, and fluctuations in the charging current all introduce error. Different hydrogen contents were obtained by various choices of charging current and charging time. It is believed that for relatively low hydrogen contents, like Charge A (250 mA-min), changing both parameters by factors of two, or even four, but not changing the product, has little effect on the resulting hydrogen content. The same cannot be said for the High Charge conditions. The resulting hydrogen content of the High Charge condition will not be proportional to the current-time product for Charge A. Hence, emphasis was placed on reproducible hydrogen contents for each set of tests, regardless of the absolute content obtained.

Baking at 150°C also outgasses hydrogen, as indicated in Section II. In setting the hydrogenation conditions for testing, a short bake was specified. The primary function of this bake is to promote diffusion of the hydrogen in the specimen and make its distribution more uniform before the start of the test. The bake also drives off some hydrogen, but the remaining hydrogen tends to outgas more slowly, thus minimizing the effect of differences in aging time at room temperature.

The vacuum extraction equipment described in Section IV was used to measure the hydrogen content in some specimens resulting from the several charging conditions used. The results are given in Table III.

TABLE III. Hydrogen Content by Vacuum Extraction

Specimen	Pressure, mm	Corrections[a]	Percent Hydrogen[b]	P_1, mm H_2	V_2, cc H_2	PPM
4340 E Charge A	0.170	Negligible	92[c]	0.170	0.123	0.71
212-B Charge A	0.302	+0.020	90.7	0.292	0.188	0.87
212 W 120,000 mA-min in 4 hr	2.06	+0.040	94.9	2.00	1.29	6.0
212 Y 120,000 mA-min in 20 hr	2.92	+0.050	95[c]	2.82	1.82	8.5
212 X. 120,000 mA-min in 20 hr, Broken, aged 2 days	2.04	+0.010	95[c]	1.94	1.25	5.8
212-B As-received	0.035	+0.005	Small[c]	<0.02	<0.01	<0.05

[a]Estimated initial losses.
[b]Remainder: helium purge gas and air inleakage.
[c]Estimated.

Since only a limited number of measurements have been made with the vacuum extraction system, no proof of their accuracy can be claimed. However, they appear reasonable when compared with values reported in the literature, and when considered in the light of the results of mechanical tests. Specimens W and Y were charged to a (current) x (time) value about 500 times as large as that for Charging Condition A. The measured hydrogen content was only ten times as great. Reciprocity was

also checked by charging W at ten times the current used for Y, although the product was the same. W showed about 85% of the hydrogen extracted from Y. The difference may not be reproducible, but the order of magnitude is clearly the same.

Two potential sources of error that have not been fully evaluated are hydrogen loss due to aging at room temperature, and due to losses during the initial pump-down period when the specimen is first placed in the vacuum system. It is hoped that the outgassing rate for cadmium-plated and baked specimens is very slow at room temperature, especially after some of the hydrogen is driven off during the bake. An effort was made to estimate the loss during pump-down by extrapolating the slope of the gas pressure buildup with time back to the time of insertion of the sample. The graph in Fig. 13 is a typical outgassing curve. Due to startup losses, about 30 microns should be added to the total pressure. Corrections are also made for in-leakage at the rate of 1/2 micron/hr.

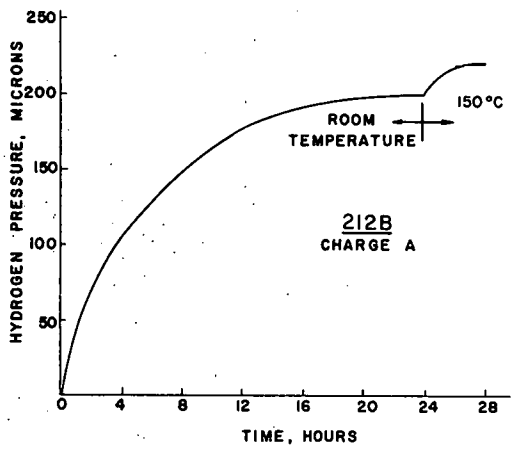

Fig. 13. Outgassing Curve; Hydrogen Pressure in Calibrated Volume as a Function of Time

The calibrated volume in the system is bound by Stopcock No. 1 and by the outlet mercury valve of the Toepler pump, as indicated in Fig. 4. Three extra expansion bulbs are available, but only one was used in this work. A 100-cc collection bulb, shown in Fig. 4, was used for sampling. Without this bulb the calibrated volume V_1 is 490 cc; with it, and its lead tube, V_1 is 596 cc.

The gas in collection bulbs was analyzed for several of the runs. Typical hydrogen content was about 95% for the High-Charge samples. The major impurity was helium from the gas bottle used to purge the system. Its contribution is larger in the other cases. The necessary corrections were made to the data.

The specimen is allowed to outgas at room temperature until the slope can be established for estimating the initial hydrogen losses. Then the specimens are moved into the furnace with a magnet and outgassed at 150°C until no further pressure increase can be detected. A 24-hr bake is used industrially to drive off hydrogen from steel, and no further outgassing was observed after 24 hr at 150°C in the system. As a check, a specimen of 4340 was charged, cadmium-plated, and baked for 55 hr, then loaded to more than 90% of its NTS and did not fail under sustained load.

There probably is other hydrogen in the steel that cannot be driven off readily at 150°C. Since this hydrogen is not readily diffusible, it does not contribute to the delayed-failure mechanism. The hydrogen of interest is the diffusible portion.

B. Dosimetry

Neutron exposures for specimens in the irradiated capsule were determined from the radioactivity of the various foil wires. Raw counting data from these wires are given in Table B-I. The activation along the iron wire that was strung axially up the center of the capsule was counted with a scanning device. Therefore absolute activities were not determined for it.

The relative activity along the iron wire is shown in Fig. 14 as the solid curve. Its magnitude has been normalized, based on the measured activities of the iron foil wires. These activities are plotted as circles according to the positions they occupied in the assembly. In addition to the iron wires, six nickel wires were used. These were activated by the reaction $Ni^{58}(n, p)Co^{58}$ with neutrons of similar energies as those that form Mn^{54}, but with a somewhat larger cross section. The nickel activities, adjusted by the ratio of the iron to nickel activation cross sections, are plotted as crosses on the same figure. At the bottom, the sketch shows the relative positions of each tier of specimens.

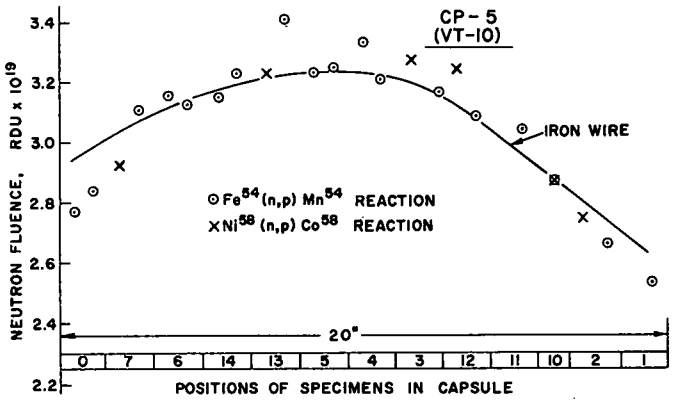

106-8825 Rev. 1

Fig. 14. Irradiation Flux Profile; Neutron Fluence as a Function of Specimen Location

The Radiation Damage Unit (RDU) is the unit used throughout this paper to report fluence (time-integrated neutron exposure). This is done with the realization that this unit is the author's own and is not in general use in the nuclear industry. However, work of the author and others in the field is leading to agreement on a unit based on the same principles that led to the development of the RDU. Until such agreement is reached, it seems prudent to use the RDU, since in the author's opinion it is the most meaningful unit available, and being clearly defined, data can easily be converted to any new unit chosen.

The RDU, its development, and its application are fully described in ANL-6826.[27] An RDU is defined as the amount of neutron irradiation that delivers the same damaging dose to an iron specimen as one fission neutron. Since large numbers of neutrons are involved, this implies a statistical distribution of neutron energies corresponding exactly to the fission neutron-energy spectrum.

The use of the RDU requires knowledge of the shape of the neutron-energy spectrum at the location of the specimen itself. Fast-neutron spectra are difficult to determine accurately, but realistic estimates, calculations, or even guesses can be made. In this case, the spectrum was calculated using multigroup reactor-physics techniques. The spectrum is tabulated in Appendix B, which begins with a brief description of the CP-5 reactor and the facility VT-10 used for the irradiations.[32] Table B-II lists the significant activation ratios, and measured and calculated activation rates. Table B-I presents the data necessary to compute the fluence.

The fluence, in RDU, is calculated below for the center of tier 5 of specimens, based on the activation of iron foil wires 5T and 5B. All other exposures can be ratioed directly from this value by the relative flux profile.

Activity of iron wire (at counting time) = 1.983×10^4 dps/mg

Correction for decay during irradiation 0.970

Correction for decay until counting 0.644

(6.2278×10^{13})(dps/mg) = Active atoms $Mn^{54}/10^{24}$ Fe^{54} atoms

RDU/Fe^{54} activation = 16.38 (Table B-II)

$$\frac{(1.983 \times 10^4)(6.2278 \times 10^{13})(16.38)}{(0.970)(0.644)} = 3.24 \times 10^{19} \text{ RDU.}$$

In Fig. 15, the results of tensile tests on various specimens of 212-B are plotted against the relative fluence of the notched region of the specimens. An approximate relationship between fluence and tensile strength over this narrow range is obtained. The expected NTS's of those specimens that were not tested in tension are indicated by the squares. These values are used for comparison purposes in the discussion of stress-rupture test results.

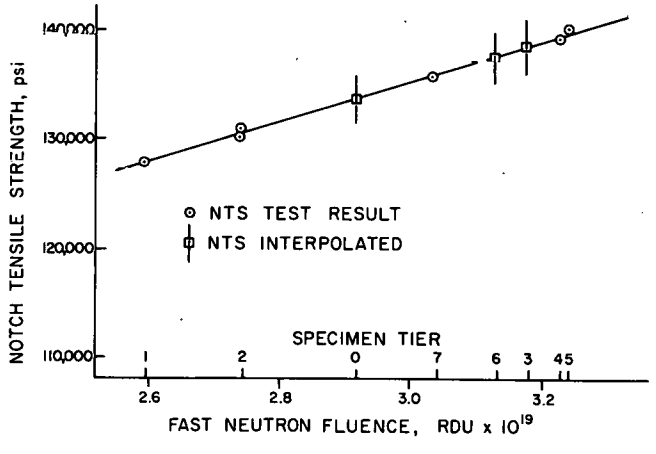

106-8826 Rev. 1

Fig. 15. 212-B Notch-tensile Strength vs Neutron Fluence

One reason for dosimetry was to verify the rise in the ductile-brittle transition temperature of the 212-B. Although there was no room to include a set of Charpy impact specimens in the capsule, this was felt to be quite unnecessary, since the rise could be computed by comparing the fluence with that in previous work on irradiated 212-B. Studies by Naval Research Laboratory (NRL)[25] and one by the author[26] were used to develop Fig. 1. The data for the CP-5 fuel element

can confidently be placed within the band. This shows that the transition temperature of the 212-B was raised enough to make the steel quite brittle at room temperature. According to Fig. 14, the specimens were exposed to fluences ranging from about 2.6 to 3.2 x 10^{19} RDU, enough to raise the transition temperature of 212-B at least 110°C. The original NDT for this steel, as determined by NRL from Charpy impact data, is in the neighborhood of 0°F. Charpy specimens of this steel subjected to this irradiation would show very little impact energy at room temperature.

C. Testing of 4340 Steel

Results of all mechanical tests on 4340 are tabulated in Appendix C (tensile tests in Table C-I, and stress-rupture tests in Table C-II). The mechanical properties are summarized in Table IV. They fit the relationships developed in tests[33] of 12 different heats of 4340 between tempering temperature, hardness, TS, and NTS. This material should correspond approximately to the 270,000-psi TS material of that study.

TABLE IV. Mechanical Properties of Type 4340 Steel

0.2% OYS, psi	TS, psi	NTS, psi	Elongation, %	Reduction of Area, %	Hardness (Avg), R_C
		Control			
238,000	264,000	296,800	7.2	39	49.1
		Hydrogenated[a]			
-	Broke head	71,800	1.6	Nil	48.7
		Irradiated 3 x 10^{19} RDU			
238,000	288,000	214,000	5.5	?	48.5
		Irradiated and Hydrogenated[a]			
-	Broke head	177,000	1.1	-	48.7

[a]Charged 100 mA-min/in.^{2}, Cd plate, bake 30 min at 150°C.

The heat-treated 4340 has a tempered martensite microstructure. Micrographs were taken with and without hydrogen, unirradiated and irradiated. Figure 16 is typical. No differences in microstructure could be detected among these four conditions.

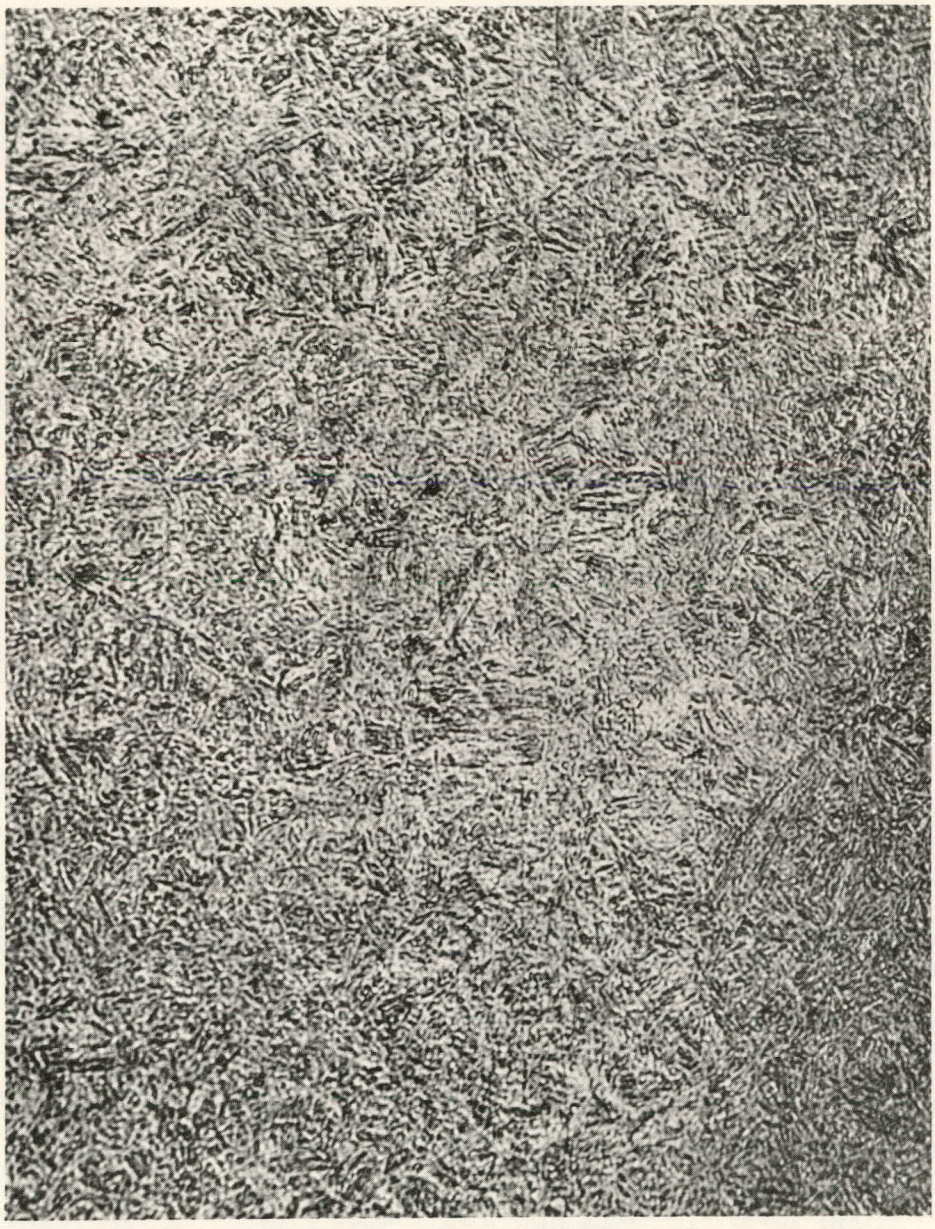

Fig. 16. Tempered Martensite Microstructure of 4340 (Etch 2% Nital, 1000X)

1. Effect of Charging Condition A

A severe charging condition was deliberately chosen for these experiments. First, a condition was sought that produces catastrophic embrittlement in 4340 in order to test the same condition for its effect on irradiated 212-B. Second, it was of interest to see if irradiation tended to reduce the sensitivity of 4340 to hydrogen enough to be evident despite a severe charge.

The work of Johnson et al.,[10] described in Section II, was used as a reference. Some of their data are reproduced in Fig. 17 to show the influence of baking time on the delayed-failure behavior. The 1/2-hr bake

is so short that enough hydrogen remains in the metal to cause very rapid failure. The open circles in Fig. 17 show results of delayed-failure tests of unirradiated specimens. The typical S-shaped delayed-failure curve does not develop because little diffusion is required to reach critical concentrations.

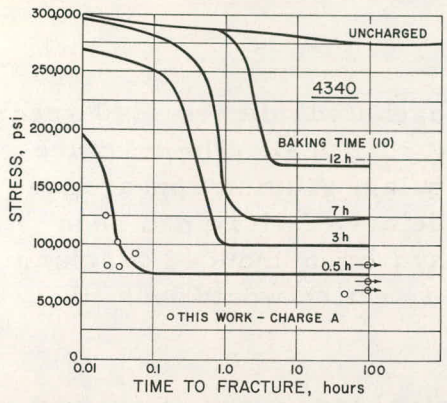

106-8827

Fig. 17. Delayed-failure Behavior of 4340 Steel Hydrogen Content Depleted by Baking,[10] Compared with Results of This Study

Condition A is even more severe than Johnson's for two reasons. First, the addition of sodium arsenate "poison" to the charging solution increases the hydrogen absorption of the specimen. Second, this material has 264,000 psi tensile strength, compared to 230,000 psi; hence it has even less tolerance for hydrogen. The result is delayed-failure times in same range, about 0.02 to 0.04 hr, but the LCS is down near 50,000 psi, two-thirds of Johnson's LCS for 1/2-hr bake time.

2. Tests of Unirradiated 4340

Figure 18 presents stress-strain curves for unirradiated material. Charging with hydrogen to Condition A caused catastrophic embrittlement, with severe strength losses in the tension test. Charged shaped and notched specimens failed with almost no deformation, at stresses well below the tensile strength of the controls.

Uncharged 4340 does not fail in stress-rupture tests at loads as high as 90% of the NTS. However, Charging Condition A reduced the NTS to about 72,000 psi. Loads above that equivalent to the NTS of charged specimens caused instantaneous failure. Delayed failures were observed at lower loads: Specimen F failed in 53.7 hr at 100-lb load (56,680 psi), but N did not at 110 lb. The LCS for this material is probably around 50,000 psi for Charge A.

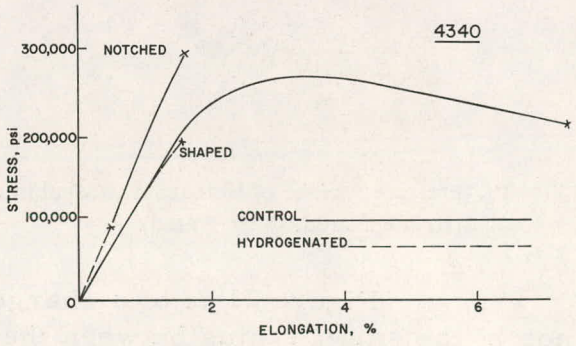

106-8831

Fig. 18. Engineering Stress-Strain Curves of Unirradiated 4340

All these specimens were cadmium plated to reduce outgassing of hydrogen during aging and testing. In most cases, tests were started the same day, but specimen M was aged 6 days before testing and it broke as expected for Charge A. To check the effect of cadmium plating, specimen L was not charged, just plated and baked. It did not fail in 100 hr at 90,000 psi. Specimen B was baked 55 hr and performed like uncharged material. All the variations observed between various tests due to

differences in preparation are consistent with the quantitative nature of the hydrogen embrittlement mechanism.

3. Fracture Appearance

Figure 19 is a photograph of a hydrogenated notched 4340 specimen. The broken control specimens look almost identical. The fracture surface is quite flat, and it has a somewhat granular, grayish appearance. This specimen was broken in a tensile test. If delayed failure had been involved, a dark ring marking the extent of the hydrogen-induced cracking in from the surface could be seen.[10] The central section would look like the fracture surface of Fig. 19.

Figure 20 is of a shaped (E-type) control specimen. It showed about 7% total elongation at 38% reduction of area, and its stress-strain curve appears in Fig. 18. The specimen failed in a cup-and-cone formation at an angle that indicates some shearing. The material is quite ductile despite its high hardness and strength.

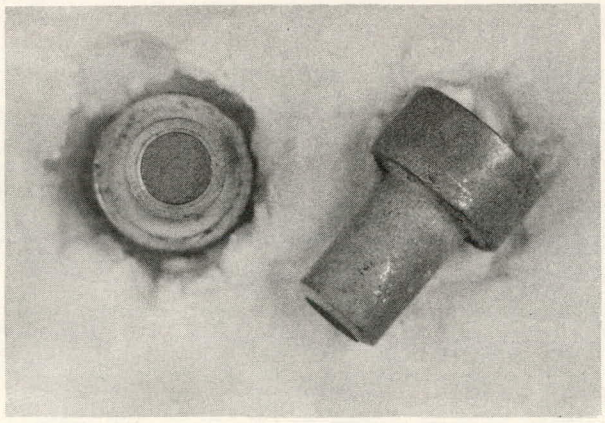

Fig. 19. Fracture Surface of Notched 4340 Specimen (Hydrogenated, Unirradiated)

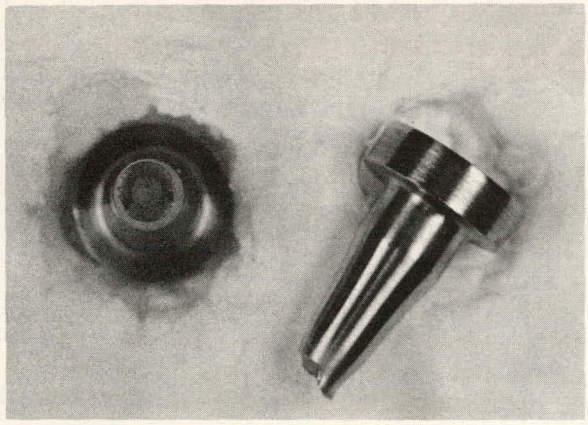

Fig. 20. Fracture Surface of Shaped 4340 Specimen (Control)

Figure 21 is of a charged E-type specimen. Because there is no notch, the small radius between the head and the body formed a stress raiser and the fracture took place under the head. It was completely brittle, and hydrogen was clearly the cause. (The mark on the end of the barrel is from a pencil; it is not a fault in the material.)

4. Tests of Irradiated 4340

Tensile behavior of the irradiated 4340 is depicted in Fig. 22. Despite the original high strength of the material, exposure to neutrons raised the tensile strength. The increase is no surprise for it is known that 4340 can be tempered to give tensile strengths as high as 290,000 psi. However, notched specimens failed at stresses well below the NTS of controls.

The only irradiated 4340 notched specimen to be tested on the Instron (where strain measurements could be made) was 0 13 ::, and it had been charged with hydrogen. One would not expect any significant elongation in this material (the controls break at 1.5% elongation), but no stress-strain curve was made for a 4340 specimen as irradiated. Results are included in Table IV.

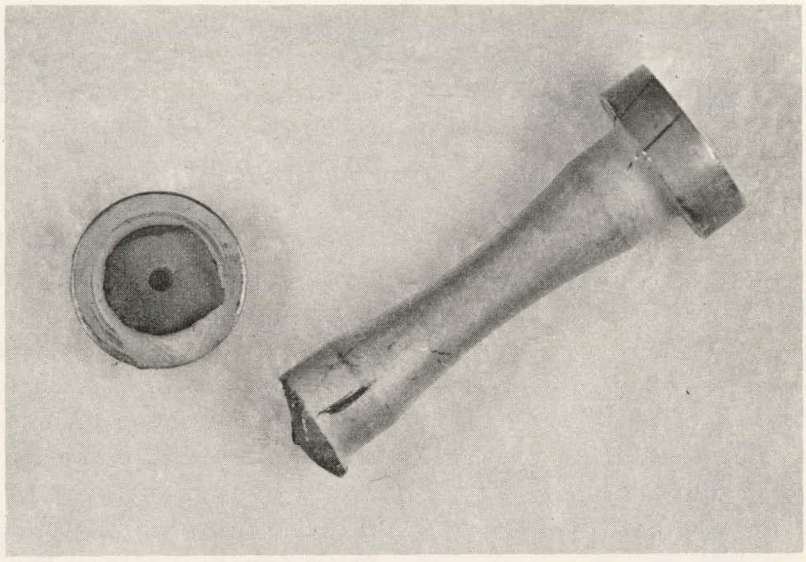

Fig. 21. Shaped 4340 Specimen, Unirradiated, Charge A. Specimen broke under head in tensile test.

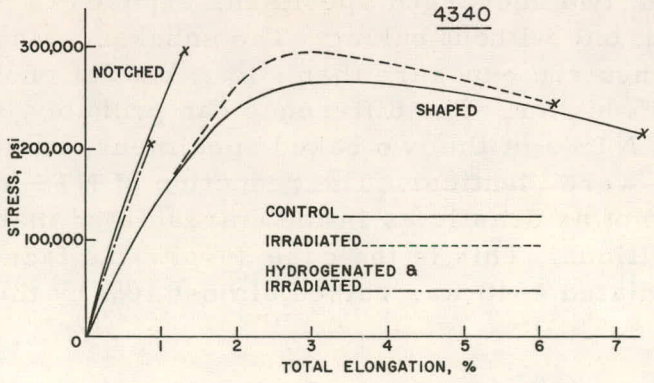

Fig. 22
Engineering Stress-Strain Curves of Irradiated 4340

The bar chart of Fig. 23 shows the results of tensile tests for both unirradiated and irradiated 4340. The tensile results for irradiated 4340 show:

a. The NTS has been reduced by the irradiation.

b. The NTS is not as drastically reduced by Charging Condition A as it is for unirradiated specimens.

c. Baking 1/2 hr lowers the NTS about 10 to 15%, both for as-irradiated and for Charge A specimens.

d. The stress-strain curve of the hydrogenated notched specimen follows that of the controls, but failure occurs sooner. (This is probably the case for the shaped specimen as well, but no strain values were obtained. It broke under its head, just like the unirradiated charged E-type specimens.)

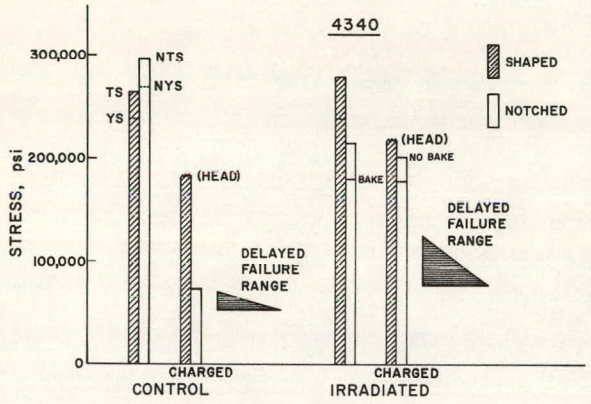

106-8833

Fig. 23. Summary Chart of Tensile and Delayed-failure Behavior of 4340

Four of the nine notched irradiated 4340 specimens were used to establish the NTS's indicated in Fig. 23. Charge A includes the 30-min bake at 150°C. A specimen ·13 .·. was charged using Condition A, and another from the same tier, 0 13::, charged identically, but not baked. One would expect the bake to drive off hydrogen, thus giving a higher NTS. On the contrary, the baked specimen had a lower NTS. It is conceivable that the difference could represent scatter only, but the charging conditions were carefully controlled and the irradiation exposures were identical. Perhaps the more uniform distribution established by the bake was more conducive to failure.

For comparison, two uncharged specimens exposed to the same neutron fluence were tested, one without baking. The unbaked specimen, 0 14 ·, had a slightly lower neutron exposure than : 13 :: but not enough to explain that its NTS was 15% higher. The difference can probably be attributed to the bake. The NTS's of the two baked specimens, one charged, one not, both baked 30 min, were identical. The reduction of NTS by hydrogen is reproducible, but is not as drastic as in the unirradiated material for the same charging conditions. This is the case despite the fact that the tensile strength of the irradiated 4340 was raised almost 10% by the irradiation.

In Fig. 23 the delayed-failure range is suggested by the shaded triangle. It is very shallow for the unirradiated material, simply because the charged NTS is so low, and specimens fail almost instantaneously at loads above the charged NTS. A test result is not considered delayed failure if the load is greater than that for the NTS. Based on meager evidence, it appears that the delayed-failure range is broader for irradiated 4340. The lower critical stress may be a bit higher.

An explanation based only on the fact that the irradiated NTS is less is in line with these results. There are no data that prove a trapping mechanism is involved, nor are there any that rule trapping out.

An effort was made to select a few conditions to compare against data in Fig. 17. The predictions and results are presented in Table V. These few data show that irradiated 4340 is still sensitive to hydrogen, and the diffusion mechanism for delayed failure still functions. There are too many variables and too few points to draw further conclusions.

TABLE V. Delayed-failure Behavior of Irradiated and Charged Type 4340 Steel

Idcnt.	Charge	Bake, hr	Stress, psi	Time to Failure Predicted from Fig. 17, hr	Time to Failure, hr	Comments
0 12:	A	0.5	79,340	0.1	10.8	LCS at 5% less load
0 12::	A No poison	6	158,700	0.8	Inst.	89% NTS
·12·:·	A No poison	3	102,000	1-100	8.8	At LCS
·11·:	A	0.5	90,690	0.03	0.03	
·11::	A No poison	5	113,360	1	0.03	

D. Testing of 212-B Steel

Pressure-vessel steel 212-B was tested in tension and for delayed failure. Tests were made on controls and on irradiated specimens. Two different hydrogenation conditions were used: Charge A, which was identical to that used with the 4340, and High Charge, in which the product of current and charging time was 480 times that of Charge A. The data from all of these tests are tabulated in Tables C-III through C-VI.

Figure 1 indicates that an irradiation of 3×10^{19} RDU raises the nil-ductility transition temperature for this steel about 110°C. Thus the irradiated material would show very little impact energy at room temperature. By engineering definition, the material is brittle. Table VI summarizes the mechanical properties of the 212-B control and irradiated

TABLE VI. Mechanical Properties of Type 212-B Steel

Yield Stress, psi	NTS, psi	Elongation, %	Reduction of Area, %	Hardness (Avg), R_A
		Shaped Control		
36,800	76,200 (TS)	14	48	45 ± 1
		Notched Control		
82,000	104,160	5.5	18	
		Notched Irradiated: $2.6\text{-}3.2 \times 10^{19}$ RDU		
100,000	128,800	2.5	~5	54 ± 2
115,000	140,200			

material. The changes in ductility, hardness, and tensile properties are as expected for this fluence. The two lines of irradiated-test data represent the maximum and minimum fluence levels.

Table III indicates that the total diffusible hydrogen content in the 212-B for the Charge A condition is about 0.87 ppm. The High Charge condition yields a content of 8.5 ppm. The amount of diffusible hydrogen in an uncharged specimen is negligible, and difficult to measure with the accuracy limitations of the system.

Photomicrographs were taken of samples from each condition. At a magnification of 1000, no differences were visible among any of the pictures. Figure 24 is a typical micrograph of the ferrite-pearlite structure of this steel.

1. Effect of Hydrogen on Unirradiated 212-B

Charging Condition A does not yield a very high concentration of hydrogen in the 212-B (less than 1 ppm). The shapes of the stress-strain curves are not substantially affected, although the values obtained for TS and NTS show a clear and reproducible reduction. The High Charge condition changes properties in a similar fashion, but there is enough difference in the curves to be significant.

Figure 25 shows the effect of the two charging conditions on tensile tests of shaped specimens. The large elongation (about 18%) for the Charge A specimen is probably more typical of control material than the curve marked "Control," but at such high elongations scatter of data is likely. However, the High Charge resulted in a loss of half the elongation and almost three-fourths of the reduction in area, in addition to the reproducible reduction in tensile strength.

Figure 26 shows the large elongation and the typical cup-and-cone type fracture of the control material. Figure 27 is of a High Charge E-type specimen. The fracture surface is extremely jagged as if it had been torn apart in many different regions before the final failure occurred.

The shapes of the Charge A curves for notched specimens are so little different from the control curves that they have been omitted from Fig. 28 for clarity. The High Charge causes the notched specimen to lose about half of its elongation, and almost all of its reduction in area. As in the case of the shaped specimens, the NTS is reduced in some direct proportion to the hydrogen content. Enough tests were run to assure the reproducibility of the data.

A set of photographs shows the fracture surfaces of these specimens. Figure 29 shows the jagged surfaces of a control specimen. Figures 30 and 31 are for Charge A and High Charge, respectively.

Fig. 24. Photomicrograph of 212-B Typical Ferrite and Pearlite Microstructure (Etch 2% Nital, 1000X)

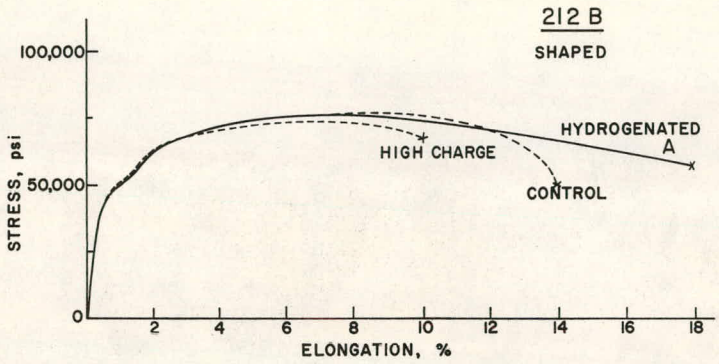

106-8834

Fig. 25

Engineering Stress-Strain Curves of Unirradiated 212-B Shaped Tensile Specimens

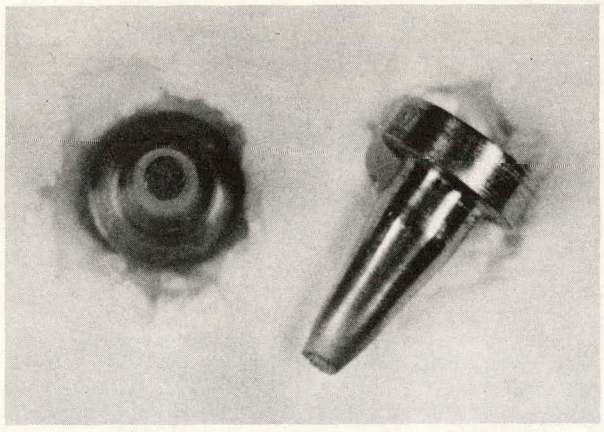

Fig. 26. Fracture Surface of Shaped 212-B Specimen (Control); Cup-and-Cone Fracture

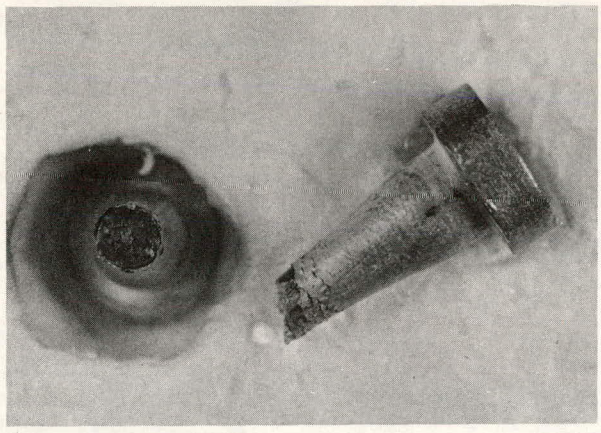

Fig. 27. Fracture Surface of Shaped 212-B Specimen E-V (High Charge)

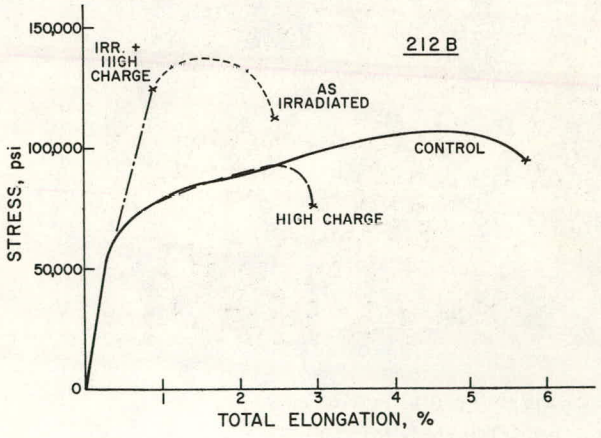

106-8836

Fig. 28. Engineering Stress-Strain Curves of 212-B Notched Tensile Specimens

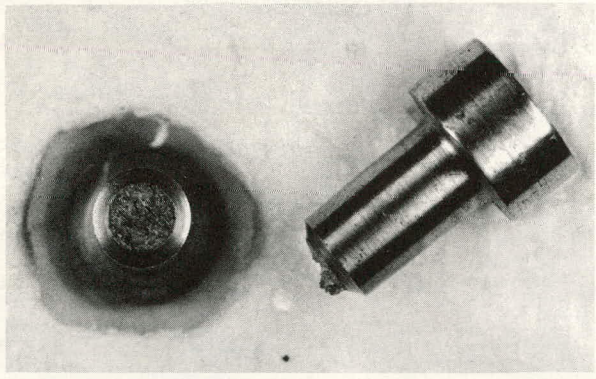

Fig. 29. Fracture Surface of Notched 212-B Specimen (Control, Unirradiated); Tensile Test

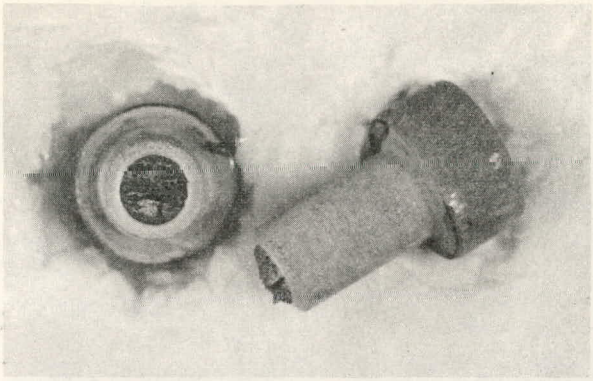

Fig. 30. Fracture Surface of Notched 212-B Specimen D (Charge A Unirradiated); Stress-Rupture Test

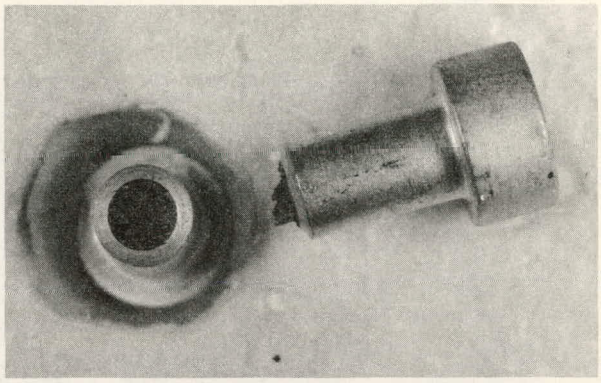

Fig. 31. Fracture Surface of 212-B Notched Specimen X (High Charge, Unirradiated); Stress-Rupture Test

The small spot of shiny intergranular fracture surface in the Charge A specimen (Fig. 30) is there because that specimen was broken on loading in a stress-rupture test. The load was too great to allow an incubation period and delayed failure, and the effective loading rate was quite high; thus the small brittle region appears. A similar broken face is shown at higher magnification in Fig. 32.

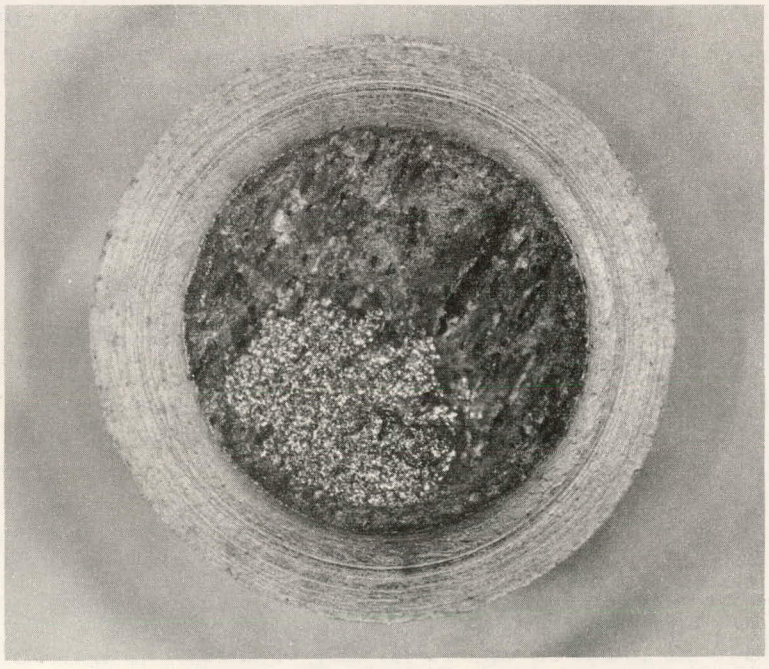

Fig. 32

Fracture Surface at High Magnification (Charge A, Unirradiated); 212-B Notched Specimen

Figure 33 is also a High Charge specimen, but at high magnification, and the fracture surface is so jagged that parts of it are out of focus. The hydrogen must cause the cracking that leads to this type of fracture surface.

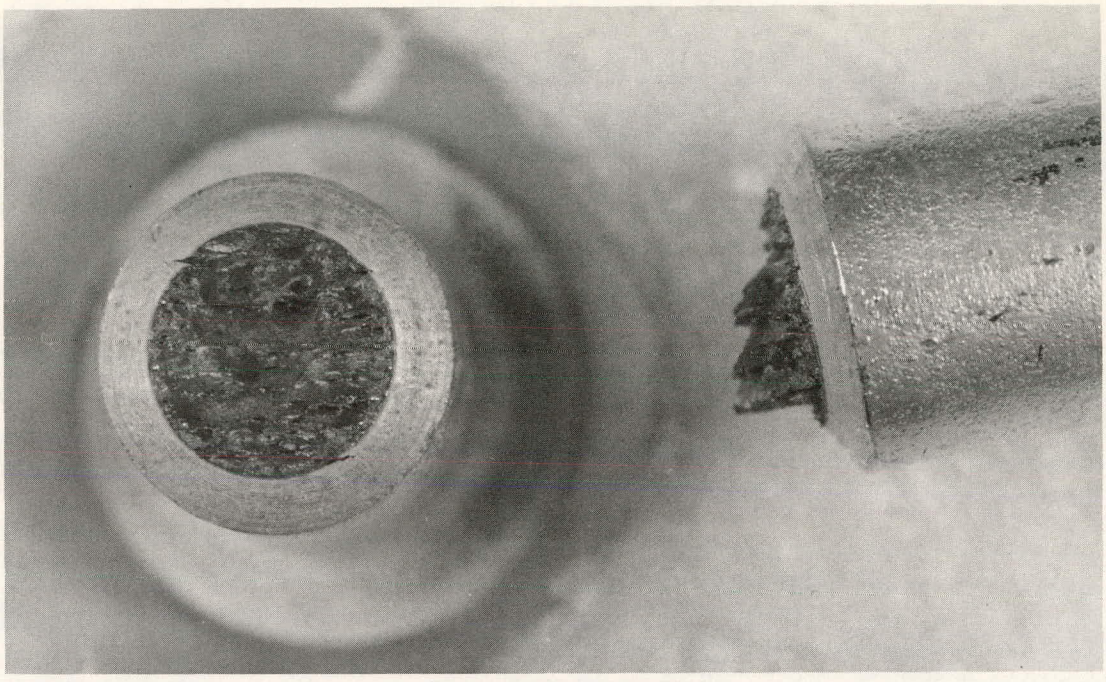

Fig. 33. Fracture Surface at High Magnification (High Charge, Unirradiated); Specimen X of Fig. 31

Evidence of embrittlement due to hydrogen is found in comparing the ratio of NTS to TS for the three conditions. Taking data from Table C-III and averaging gives:

	NTS/TS
Control	1.37
Charge A	1.34
High Charge	1.26

For an ideally ductile steel, this ratio would approach 1.5. The more brittle the steel, the nearer the ratio is to unity. Hence, putting enough hydrogen in the steel definitely reduces its ductility. There were no shaped specimens of 212-B in the irradiation capsule; therefore this comparison cannot be made for the irradiated material.

2. Effect of Hydrogen on Irradiated 212-B

The increase in the NTS of 212-B due to this irradiation was shown in Fig. 15; Table VI shows this increase to be from 22 to 34%. The difference in flux over the length of the capsule (see Fig. 14) is enough to produce a significant spread in neutron fluence. This difference of about 20% in flux results in a spread of about 9% in NTS. Over this fairly short range, the dependence of NTS on RDU (shown in Fig. 15) is practically linear.

Since the variation is only 9%, the general behavior of all the irradiated specimens is similar. It will be convenient for analysis to normalize all the stress levels involved to the NTS for the particular tier of specimens being considered. Thus, steels irradiated in the range of 2.6 to 3.2 x 10^{19} RDU can be discussed as a set, without further comment on the spread (not scatter) of data due to the flux profile. For tiers 3, 6, and 0, no tensile test was made of a specimen as irradiated. The NTS for those specimens was interpolated from Fig. 15.

Figure 28 is the stress-strain curve for a typical irradiated notch-tensile specimen. This one came from tier 7 in the capsule, about midway in exposure between the highest and lowest. The others would look similar, with the elongation to fracture being less as the NTS is increased.

Figure 28 shows the effect of the High Charge. With this specimen, the same curve was developed through the elastic range, but it broke before the onset of plastic flow. This type of behavior was reported by Hobson and Sykes,[34] who charged a chromium-molybdenum steel and then allowed different specimens to age longer than others. In this way they got a broad range of hydrogen contents. Their tensile test results, plotted as true stress vs true strain, all fall on the same curve. The longer the age, the further along the curve before failure.

It has been argued that some plastic flow at the root of the notch must take place before delayed failure. The behavior of this irradiated specimen might be cited in an effort to refute this, but the simple fact that the failure took place in the elastic part of the curve is not proof. In fact, in this test, the failure could have taken place just as soon as a little bit of plastic yielding occurred. The curve is almost at the yield point, so once a little flow takes place, the stress on the remaining material under the notch root is suddenly increased. For an irradiated and hydrogenated specimen, the remaining material is brittle, and the crack propagates rapidly.

Pictures of the fracture faces of irradiated 212-B show an interesting contrast. Figure 34 shows a specimen that was broken in delayed failure, but not hydrogenated. Most of its fracture surface is brittle, as

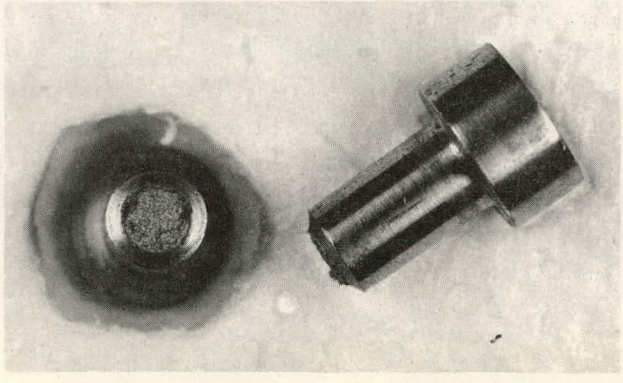

Fig. 34

Fracture Surface of Irradiated 212-B Specimen 3 (As Irradiated); Stress-Rupture Test

would be the case for the same material broken in tension. This specimen produced the "as-irradiated" curve of Fig. 28. Figure 35 shows the results of a tensile test of an irradiated specimen with Charge A. There is a thin dark ring at the notch root, and the rest of the broken surface has a typical brittle appearance. Figure 36 is of the specimen discussed in the preceding paragraphs, irradiated and hydrogenated, and tested in tension as indicated in Fig. 28. It looks like a flat brittle fracture, with none of the jagged appearance of the High Charge control specimens. The combination of high hydrogen content and irradiation-embrittled steel results in a fracture that looks granular, suggesting that a crack would propagate rapidly once initiated in such material.

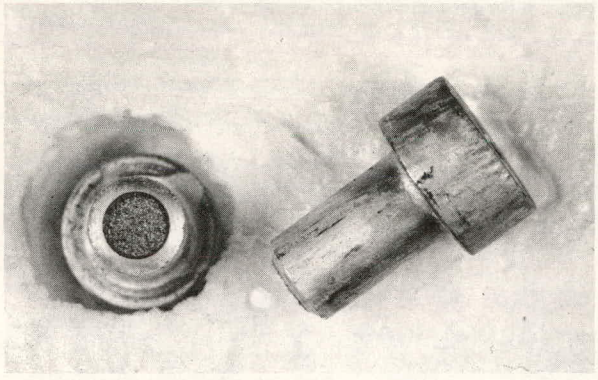

Fig. 35. Fracture Surface of Irradiated 212-B Specimen 5 (Charge A); Tensile Test

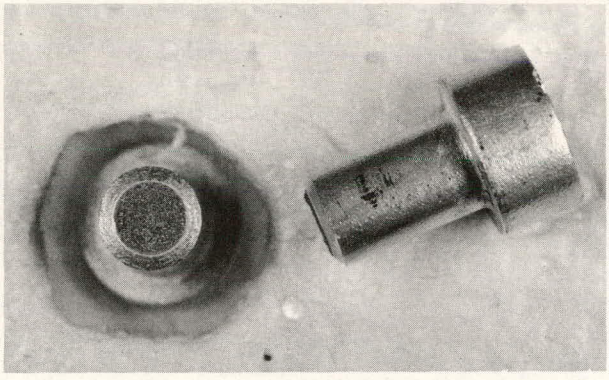

Fig. 36. Fracture Surface of Irradiated 212-B Specimen 7 (High Charge); Tensile Test

3. Delayed-failure Characteristics

A notched specimen will ultimately fail under constant load at stresses somewhat below the NTS. This behavior is observed without the presence of hydrogen, but generally speaking, the stress levels are above 90% of the NTS of the material.

Stress-rupture tests were run on control and as-irradiated material to try to determine the lower critical stress as a function of the NTS. Similar tests were conducted on specimens charged with hydrogen, both for Charge A and for the High Charge. The data are given in Tables C-V and C-VI. They are correlated by plotting the applied stress as a percent of the unhydrogenated NTS for each test, as in Fig. 37.

In Fig. 37, the NTS of a hydrogenated specimen is indicated by a square, as a percent of the unhydrogenated NTS. Thus, under Charge A Unirradiated, a square shows that the charged NTS was about 96% of the uncharged NTS. The time to failure in hours is indicated for each stress-rupture test. An X indicates a test that did not fail in 100 hr. The lower critical stress must be above the X for a given condition.

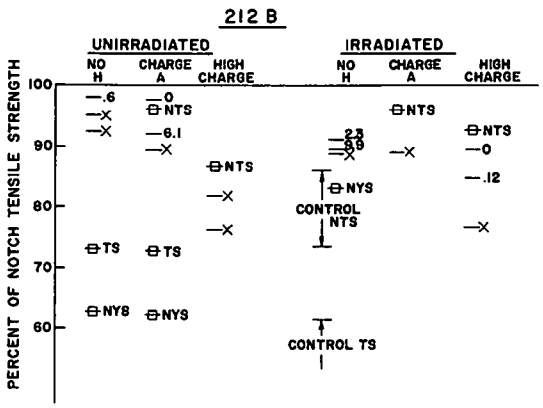

106-8829

Fig. 37

Correlation of Tensile and Stress-Rupture Test Results for 212-B; Applied Stress as a Percent of Unhydrogenated NTS

A trend can be discerned from these results. In each case, a narrow band where delayed failure is observed is between the NTS and the LCS. The band is broader for steels with higher strength level or heavier hydrogen charge. However, the delayed-failure range of stresses seems to be between about 90 and 95% of the charged NTS for the same charging condition. In no case is the catastrophic loss of strength, so typical of hardened 4340, observed.

From the few points available, the LCS was determined as a function of neutron fluence. Figure 38 is based on Fig. 15, which shows the NTS as a function of the fluence. In Fig. 38, the NTS is again shown against fluence, but the comparable lines for the charged NTS results are added. The LCS values really require more data points to fix them exactly; however, with a limited number of tests, a conservative LCS can be chosen at the highest stress test that survived 100 hr of load. Even for the irradiated steel, the LCS is not much below the original NTS of the material. No delayed failures could be achieved at stresses as low as the tensile strength of the original material.

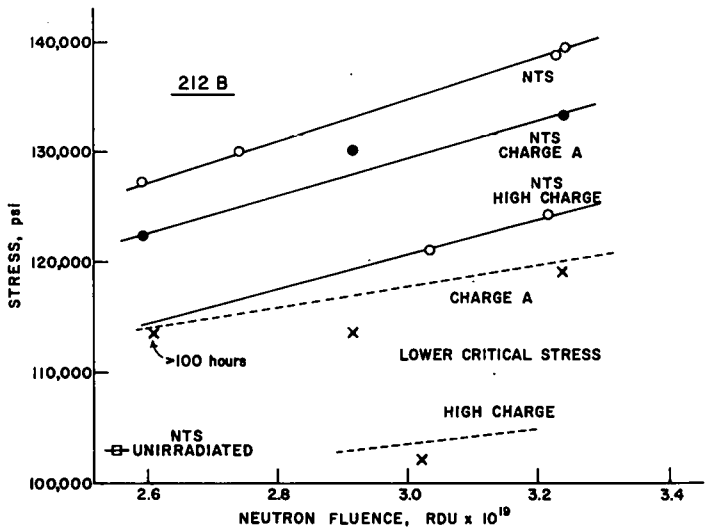

106-8835 Rev. 1

Fig. 38. Notch-tensile Strength (NTS) and Lower Critical Stress (LCS) for Irradiated 212-B with Different Hydrogen Charging Conditions

VI. DISCUSSION

A. Hydrogen in Irradiated Pressure-vessel Steels

1. Charging Condition A

Charging Condition A was chosen for study of pressure-vessel steels, not to establish a high hydrogen content, but to duplicate a known condition. Charge A produced catastrophic embrittlement in 4340, so the technique was duplicated, even though the strength level of 212-B was much lower. The comparative behavior of the irradiated steel was the real question.

The first set of mechanical tests proved there was no significant loss in properties in 212-B, except a 4% loss in TS and NTS. Delayed failure occurs only in the stress range of 90 to 95% of the NTS for the hydrogenation condition employed.

The bar chart of Fig. 39 shows this clearly. The two sets of bars on the left are for unirradiated material, and for all practical purposes, Charge A does not cause any change. The shaded triangle indicates the delayed-failure range; its base is the lower critical stress. The performance of irradiated 212-B is shown on the right side of the chart. It was stated in Section V that this steel is brittle at room temperature due to the effect of the neutron bombardment. The fracture surface of the irradiated material verifies its brittle condition. However, irradiated specimens charged to Condition A show no particular effect attributable to hydrogen. It is evident that Charge A does not introduce enough hydrogen into 212-B to cause significant embrittlement.

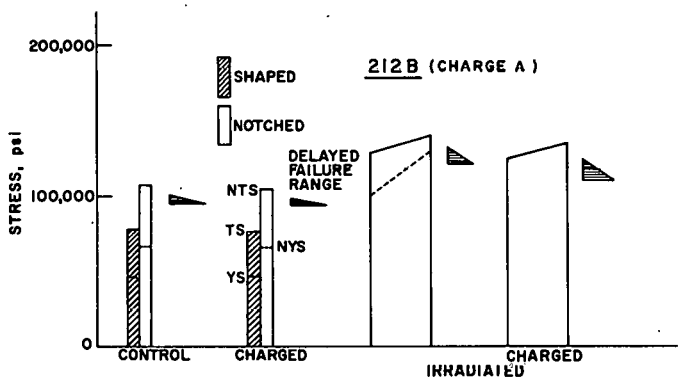

106-8837

Fig. 39. Bar Chart Showing Mechanical Behavior of 212-B for Charging Condition A

Vacuum-extraction analysis indicated that the hydrogen content of these test specimens is about 0.9 ppm. This is typical of the concentrations calculated as being possible for a thick, unclad pressure vessel. Harries and Broomfield concluded that the primary source of hydrogen in such a vessel would be corrosion by the reactor water.[35] They give equilibrium concentrations for various water temperatures and vessel wall thicknesses, and these concentrations range from less

than 0.1 to 1.3 ppm. The Westinghouse analysis,[29] mentioned previously, suggests this range for operating conditions, and about three times as high after prolonged shutdown.

Hydrogen contents of this order are not sufficient to cause deterioration in properties of vessel steels in their design stress range. No difference in performance at stresses below the yield stress could be expected.

2. High Charge Condition

The High Charge condition was selected because it caused a significant loss in mechanical properties of the 212-B. It is far more severe than that necessary to completely embrittle high-strength steels and is twice as high in mA-min (charging current x time) than the condition used by Cain and Troiano[19] to embrittle normalized steel. At these currents and times, reciprocity breaks down and the resulting hydrogen content is not proportional to mA-min. Based on vacuum extraction, these High Charge specimens contained about 8 ppm hydrogen. This is more than one would expect to find in practice due to any corrosion reaction. In any system that operates at elevated temperature, this concentration could never be maintained, because the hydrogen would quickly diffuse out.

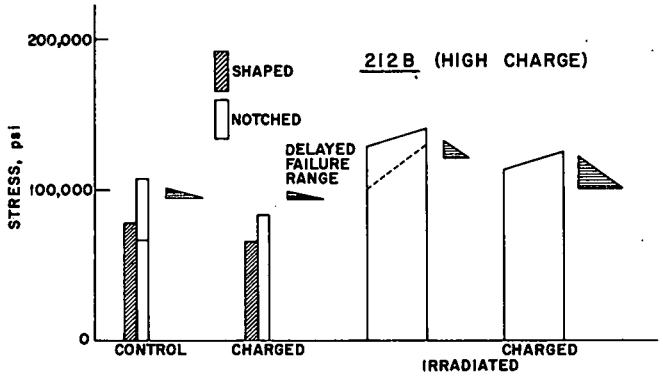

106-8838

Fig. 40. Bar Chart Showing Mechanical Behavior of 212-B for High Charge Condition

However, this condition was chosen to see how irradiated steel would perform with a high concentration of hydrogen. Figure 40 is a bar chart like Fig. 39. In fact, the charts are very much alike, the only difference being in the magnitude of the strength loss due to the high hydrogen content. Most important, the delayed-failure range remains roughly the same.

The most important concern is whether the irradiation-hardened steel could suffer a catastrophic strength loss due to hydrogen, like that observed in the high-strength steels. These tests showed that even the irradiated steels can maintain an LCS of above 75% NTS for these hydrogenation conditions. This is not considered "catastrophic embrittlement."

These results are compared with those of Cain and Troiano[19] in Fig. 41. They studied a pearlitic 4620 steel for application in a hydrogen sulfide environment. Delayed failure in about 0.2 hr was observed,

as shown by the dots in Fig. 41. The charging conditions approached the High Charge condition of this work. A lower critical stress of 100,000 psi, or about 68% NTS was found. This steel had a TS of 100,000 psi and a NTS of 150,000 psi. This is slightly higher than the strength range of the irradiated 212-B tested. Despite the High Charge and the fact that the irradiated 212-B steel was brittle, no sharp dropoff or great reduction in its LCS was observed. In fact, the LCS is about 80% of the NTS.

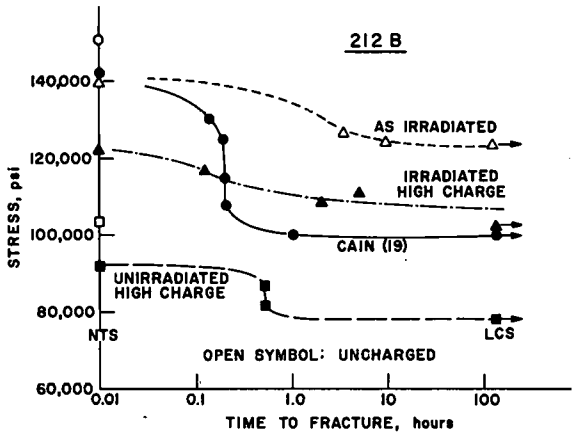

106-8830

Fig. 41. Delayed Failure of High Charge 212-B Compared with Results of Cain[19]

In all of the studies of 212-B that were highly charged, the stress range from the charged NTS down to the LCS was about the same. The hydrogen content is sufficient to reduce the NTS, so it must be appreciable, but further reduction in the LCS is not large. Figure 41 shows this to be the case even for the unirradiated 212-B (black squares). The irradiated data look much like those for bainite and tempered martensite having about the same strength levels.[19]

Replotting the data for High Charge specimens of 212-B, in terms of the applied stress as a percent of the NTS, suggests once again that the delayed-failure behavior is controlled by the strength level. Figure 42 is plotted in this manner. For the High Charge condition, delayed failures occur in the range between 80 and 86% of the uncharged NTS. When plotted against the NTS for the charging condition involved, the failure range is from 90 to 95% NTS. This behavior is consistent over the range of irradiated NTS values shown in Fig. 38, and over the unirradiated data as well.

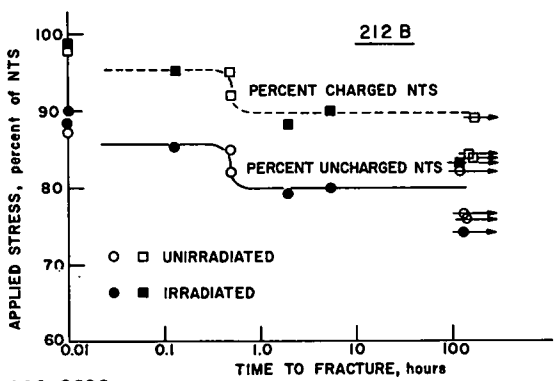

106-8828

Fig. 42. Delayed Failure of High Charge 212-B; Applied Stress as a Percent of Charged NTS

Thus, for this pearlitic steel 212-B, the pattern of the delayed-failure behavior shows a LCS at about 90% of the charged NTS. This range is typical even for uncharged specimens, as seen in Figs. 37 and 42. However, the NTS itself is lowered by hydrogen.

This behavior suggests that either the hydrogen does not diffuse as well in lower-strength steel, or if it diffuses it does not build up

critical concentrations. Actually, the triaxial stress field is limited by yielding, thus limiting the driving force for preferential diffusion. On the other hand, the critical concentration for cracking these softer and weaker steels may be very different than for hardened 4340.

The loss of NTS and the appearance of the fracture surface for High Charge specimens show that the hydrogen concentration is high to begin with, and does not require time for diffusion to make its presence felt.

Over the strength range of unirradiated to irradiated 212-B, the pattern of behavior is the same, despite the fact that the NTS of the material changes by 35%. Perhaps this is not enough difference in strength level to be important, although it is enough in quenched and tempered 4340. However, when radiation strengthens steel, it does not change the microstructure (as heat treatment would) or the grain arrangement (as cold work would). For all intents, the material is the same except for strength level, and no dependence of hydrogen influence on strength level is observed.

Table III gives the result of a hydrogen determination on specimen 212 X. Comparing with 212 W shows that a substantial amount of hydrogen remained in the specimen after a fracture that was affected by hydrogen. This indicates that only a small fraction of the hydrogen present had diffused to the region of failure and had been lost at fracture.

3. Safety of Reactor Pressure Vessels

One purpose of this study was to consider the possibility of catastrophic hydrogen embrittlement in a nuclear reactor pressure vessel. It is generally agreed that ductile steels used for reactor vessels are of low enough strength that the hydrogen concentrations needed to embrittle them are beyond reality in practice. These experiments indicate that this is the case, since even with a high artificial charge the loss in NTS is about 10%. The LCS is only another 10% below that. This is not catastrophic.

The Pressure Vessel Code requires designers to keep the maximum stress in the structure below the yield strength. It certainly means that designers can keep stress levels from reaching the failure range (>80% NTS). This is not a valid design criterion, however. Empirical tests reflect only their exact conditions, and detailed stress analysis would be required to relate these tests to design.

The literature contained no evidence as to how neutron irradiation would affect the hydrogenated tensile and stress-rupture behavior of 212-B. This work shows little effect. The reduction in NTS is about the same percentage of the NTS irradiated as unirradiated. Since irradiation increases the yield, TS and NTS, the loss due to hydrogen does not

even bring these parameters back to their original levels. The net effect is still one of strengthening, but because of the rise in NDT due to neutron embrittlement, vessels are generally not designed to operate to fluences as high as those used in this experiment, and no credit is taken for this strengthening in design.

As for hydrogen embrittlement itself, vessel designs must continue to avoid sharp corners, and be inspected to avoid cracks or flaws that could act as stress raisers. Next, the processes by which hydrogen enters steel must be studied so that hydrogen content can be predicted more confidently. The critical local concentration, not the average hydrogen content, can cause failure. Nevertheless, the mechanisms of entry must be known to make limiting analyses.

Harries and Broomfield[35] considered dissociation of hydrogen from water at the vessel inner surface, radiolytic decomposition, and the corrosion reaction as potential hydrogen sources. The latter furnishes most of the hydrogen. The vessel thickness and temperature determine the equilibrium distribution and they predict a maximum of 1.5 ppm in a 10-in. vessel at 250°C.

Harries and Broomfield's analysis is for an unclad vessel, so that a cladding failure is not expected to produce unusually high hydrogen contents in a clad vessel.

As long as these concentrations are in the 1- to 2-ppm range, the necessary conditions for catastrophic delayed failure do not exist in 212-B reactor pressure vessels.

B. Questions on Behavior of Irradiated Steel

With the influence of strength level so clearly shown by tests on 4340 and other high-strength steels, it is surprising to find no change in behavior pattern of 212-B as its strength is raised by irradiation. Perhaps at these low strength levels the effect is masked. It may be that another factor of 4 or 5 in exposure would produce a different pattern. There is no reason to expect a different microstructure as a result of irradiation, as contrasted with tempered martensite, where the tempering temperature determines the final structure and the mechanical properties.

Irradiated 4340 raises other questions. The NTS was reduced, although the TS rose. After irradiation, the steel was still subject to delayed failure after charging, although Charge A no longer resulted in as great a strength loss. Irradiated 4340 is much more notch-sensitive than its quenched and tempered control. In fact, the NTS/TS ratio is well below unity. The reason for this behavior is not apparent.

C. Future Work

During these experiments, certain problems or possible methods of attack on existing problems have come to mind. A few are listed below.

1. More experiments are needed on the effect of irradiation on nonequilibrium, heat-treatable, high-strength steels. Their sensitivity to hydrogen after irradiation should be interesting to evaluate quantitatively if the drop in the NTS of 4340 observed here is typical.

2. The damage caused by neutron irradiation in steel tends to anneal out in the temperature range starting about 250°C. This has been observed in many experiments. Since a diffusion mechanism is involved, there may be a temperature range where catastrophic delayed failure due to defect diffusion and local buildup could take place under sustained load.

3. Although the strain rates are very high, impact testing of highly charged pressure-vessel steels may show a loss of impact strength due to hydrogen.

4. Work is needed on more realistic ways to determine the amount of hydrogen that could accumulate in reactor pressure-vessel walls.

5. The permeation and diffusion rates for hydrogen in pressure-vessel steel are needed. They should be measured as a function of temperature, and companion measurements on 4340 should be carried out for comparison.

6. The type of neutron-diffusion calculations used for reactor design might be adaptable to the study of the preferential diffusion of hydrogen in steel.

7. When powerful enough neutron beams become available, neutron diffraction might be used to find the interstitial location of hydrogen in the iron lattice. Deuterium would have to be charged into iron highly enriched in the Fe^{54} isotope to obtain adequate resolution.

8. Continued work on vacuum extraction for hydrogen determinations is justifiable. Errors must be evaluated. The range of validity of the reciprocity law for electrolytic hydrogen charging should be studied.

9. If only a small fraction of the contained hydrogen escapes at fracture, perhaps tritium could be used to determine the amounts involved. The difference in fraction released tensile testing and delayed-failure testing could indicate the extent of concentration by diffusion.

10. Since the High Charge 212-B shows strength loss in the tensile test, studying this as a function of straining rate would be worthwhile. The range should extend from impact tests to delayed-failure work.

VII. CONCLUSIONS

1. Delayed failure due to hydrogen can occur in lower-strength steels like 212-B, but the LCS did not drop below 75% of the uncharged NTS, even with the high hydrogen content used.

2. Charging 212-B with hydrogen results in a lowering of the NTS itself. The amount of lowering is a direct function of the hydrogen content.

3. Delayed-failure tests reveal a LCS at about 90% of the charged NTS for 212-B, independent of the strength level.

4. The above characteristics are observed in 212-B irradiated to 3×10^{19} RDU in which the NDT has been raised to 90°C above room temperature. Irradiation raises the NTS, and the hydrogenated results are changed in proportion. Irradiation does not change the microstructure.

5. Even if a mechanism were available for building up hydrogen in a reactor pressure-vessel wall, the conditions for catastrophic delayed brittle failure do not exist in practice.

6. The lower-strength steels are not as susceptible to delayed failure because the stress intensities necessary for adequate preferential diffusion cannot be maintained. Triaxial elastic strain is essential, and the lower-strength steels yield before such diffusion can take place.

7. Delayed failure occurs in as-irradiated 212-B, but the pattern is comparable to the control and charged material.

8. Irradiation raises the TS of irradiated 4340, but it reduces the NTS. Catastrophic delayed failure still occurs, but the hydrogen appears less effective for a given charge condition.

9. The amount of diffusible hydrogen in a steel sample can be determined by vacuum extraction at 150°C. Only a portion of it is released when the specimen breaks.

APPENDIX A

Materials

1. Pressure-vessel Steel SA 212-B

This material was processed and fabricated in such a manner as to be similar in analysis and properties to the United States Steel Corporation (USS) standardized heats of material. Characterization was accomplished at the USS Research Laboratory in Monroeville, Pennsylvania.

The SA 212-B material was produced by the open-hearth process with the use of fine grain practice. Ingots were formed into slabs 11 in. thick. The chemical analysis is given in Table A-I.

TABLE A-I. Chemical Composition of Steels, Percent

	212-B	4340		212-B	4340
C	0.25	0.39	Ni	0.018	1.71
Mn	0.69	0.80	Cr	0.045	0.82
P	0.022	0.013	Mo	<0.005	0.21
S	0.029	0.018	Al	0.017	*
Si	0.18	0.26	N	0.005	*
Cu	0.022	*	B	*	0.00005

*Not determined.

Fabrication of the slabs to plate was witnessed by Naval Research Laboratory personnel. In accordance with specifications, the plates were cross-rolled to obtain as nearly as possible a 1:1 rolling ratio. All chemical analyses and mechanical testing were done according to ASTM Designation: A212-61T and ASTM Designation: A20-59 specifications.

After being rolled and before being cut into approximately 2- by 3-ft sections for shipment, the two plates were heat-treated according to the specifications. The heat-treating schedule called for the material to be charged into a furnace whose temperature was 1110°F and heated at a rate of 63°F/hr to 1650°F. The material was then held at 1650°F for 1 hr per inch of thickness (4 hr) and water-quenched to 300°F. It was then to be recharged into a furnace at 750°F and heated at a rate of 63°F/hr to 1175°F for 1 hr per inch of thickness and air-cooled. The material after this treatment was then in the quenched and tempered condition and ready for testing. After being heat-treated, the plate was flame-cut into sections for shipment. A heat-affected zone of at least 2 in. should be expected. Each plate was marked by metal stamping to locate its position in the original slab. These markings are along the last rolling direction. The results of mechanical-property tests are given in Table A-II.

TABLE A-II. Mechanical Properties of Quenched and Tempered 4-in. Plate of 212 Grade B Steel (Longitudinal orientation; quarter-thickness location)

Yield Strength (0.2% offset)	42,700 psi
Tensile Strength	76,000 psi
Elongation	31%
Reduction of Area	66%

Charpy V-Notch Impact Test Results

Temperature, °F	Energy Absorbed, ft-lb	Fracture Appearance, %
120	72	97
80	48	65
60	36	60
40	27	50
20	25	42
10	15	27
-20	7	10
-50	5	5

2. High Strength 4340

The 4340 was purchased from Osco Steel Company, Cleveland, Ohio, in the form of 5/8-in.-diam round bars. The material is hot-rolled and annealed, and is graded Aircraft Quality, AMS-2301. The composition is given in Table A-I.

The specimens were machined from the bar stock and then heat-treated as follows:

Heated to 1550°F in vacuum furnace,
Oil-quenched,
Tempered at 550°F, 1/2 hr to reach temperature and
$1\frac{1}{2}$ hr at temperature.

A nominal tensile strength of 267,000 psi was obtained. The average Rockwell C hardness obtained on the ends of the specimens was 49.7 ± 1.1.

APPENDIX B

Irradiation Details of CP-5 Reactor

The CP-5 is Argonne's research and test reactor. It is a tank-type system, cooled and moderated by heavy water. The nominal power level is about $4\frac{1}{2}$ MW. The reactor uses 17 tubular fuel elements in its core. Each of these is an arrangement of three concentric tubes of aluminum-uranium alloy, clad with aluminum. Inside the central tube there is space for experimental irradiations. This irradiation was performed in VT-10, the vertical thimble in the center of fuel element No. 10. The capsule wall was cooled by reactor water.

The author has calculated the fast neutron spectrum in the CP-5 VT-10. In addition, the responses of different foil materials to the fast neutrons were analyzed. With this information the dosimetry reference information given in Table B-I was developed. The data were used to calculate the neutron exposures presented in Section V.

TABLE B-I. Summary of Neutron Flux and Spectrum Data

1. Reactor: CP-5, Argonne National Laboratory, Argonne, Illinois.
2. Facility: VT-10. Hollow vertical thimble in center of cylindrical fuel assembly No. 10. Core: 17 cylindrical uranium-aluminum fuel elements, D_2O coolant. Nominal full power: 4.6 MW. Data at reactor midplane.
3. Calculated Spectrum

Tabulated Multigroup Spectrum,
n/cm^2-sec per MW of Reactor Power

Group	E_L*	Φ (per MW)	Group	E_L*	Φ (per MW)
1	7.788	0.416×10^{12}	11	0.639	11.002×10^{12}
2	6.065	1.092×10^{12}	12	0.498	10.145×10^{12}
3	4.724	2.983×10^{12}	13	0.388	7.723×10^{12}
4	3.679	4.471×10^{12}	14	0.302	10.212×10^{12}
5	2.865	6.543×10^{12}	15	0.235	9.307×10^{12}
6	2.313	9.045×10^{12}	16	0.183	8.349×10^{12}
7	1.738	9.516×10^{12}	17	0.143	7.230×10^{12}
8	1.353	10.215×10^{12}	18	0.111	8.034×10^{12}
9	1.054	10.312×10^{12}	19	0.086	6.649×10^{12}
10	0.821	10.334×10^{12}	20	0.067	7.021×10^{12}

*E_L is the lower energy limit of the neutron energy group.

TABLE B-I. (Contd.)

4. Calculated Flux and Damage Production Ratios Relative to Fe^{54} activations/sec per 10^{24} atoms Fe^{54}
   - $\Phi > 3$ MeV/Fe^{54} 2.32
   - $\Phi > 1$ MeV/Fe^{54} 9.6
   - $\Phi > 0.4$ MeV/Fe^{54} 14.7
   - $\Phi > 0.18$ MeV/Fe^{54} 20.0
   - RDU/Fe^{54} 16.38
5. Calculated Foil Activation Ratios
   - S^{32}/Fe^{54} 0.72
   - Ni^{58}/Fe^{54} 1.29
   - U^{238} fiss/Fe^{54} 3.78
6. Measured Foil Activation Rates (Fast Neutrons), activations/sec per 10^{24} atoms/MW (Ref. 26)
   - Fe^{54} 2.84×10^{11}
   - Ni^{58} 4.6×10^{11}
   - S^{32} 2.24×10^{11}
   - U^{238} 1.97×10^{12}
7. Summary Damage Data

	Per MW of Reactor Power	At Full Power, 4.6 MW
$\Phi > E_i$ (E_i = 3 MeV)	6.6×10^{11}	3.04×10^{12}
RDU/sec (including 3% for thermal flux[26])	4.78×10^{12}	2.2×10^{13}

All the foil wires were unloaded from the basket with the specimens, and pieces of each were counted and weighed. The results are presented in Table B-II in dps/mg (disintegrations per second/milligram of foil metal). From this the number of neutrons that interacted with target atoms can be calculated, and from that the neutron exposure in RDU.

TABLE B-II. Fast-neutron Fluence from Foil Data

Tier	Wire	Activity dps/mg to 2/25/66	Activations/ 10^{24} Atoms	Calculated Fluence, RDU
1 T	Fe	1.550×10^4	1.494×10^{18}	2.536×10^{19}
2 T	Fe	1.631	1.572	2.668
2 B	Ni	2.372	2.071	2.742
10	Fe	1.755	1.692	2.871
11 T	Fe	1.858	1.791	3.040
12 T	Fe	1.887	1.819	3.087
12 B	Ni	2.802	2.446	3.240

TABLE B-II. (Contd.)

Tier	Wire	Activity dps/mg to 2/25/66	Activations/ 10^{24} Atoms	Calculated Fluence, RDU
3 T	Fe	1.969×10^{4}	1.898×10^{18}	3.221×10^{19}
3 B	Ni	2.830	2.471	3.275
4 T	Fe	1.960	1.890	3.206
4 B	Fe	2.032	1.959	3.324
5 T	Fe	1.983	1.912	3.224
5 B	Fe	1.971	1.900	3.225
13 T	Fe	2.081	2.006	3.404
13 B	Ni	2.789	2.435	3.222
14 T	Fe	1.972	1.901	3.226
14 B	Fe	1.925	1.856	3.149
6 T	Fe	1.909	1.840	3.123
6 B	Fe	1.926	1.857	3.151
7 T	Fe	1.897	1.829	3.103
7 B	Ni	2.528	2.208	2.924
0 T	Fe	1.731	1.669	2.832
0 B	Fe	1.694	1.633	2.771

By the use of the ratios in Part 4 of Table B-I, the flux and total neutron exposure can be expressed in terms of neutrons with energy greater than some particular energy, if this is desired.

APPENDIX C

Tensile and Stress-Rupture Test Data

The data taken in mechanical tests are tabulated in this appendix for reference. Tables C-I and C-II give the tensile and stress-rupture results, respectively, for Type 4340 specimens. Tables C-III through C-VI are for the Type 212-B specimens.

TABLE C-I. Tensile Tests of Type 4340 Steel

Type	Ident.	H[a] Charge, mA-min	Machine[b]	Maximum Load, lb	Load at Failure, lb	Stress at Maximum Load, psi
E	0	-	B	9,550	7560	263,940
E	0	-	B	9,550		263,940
J	11	-	B	10,740	c	296,850
E	IV	-	I	9,320	7315	264,000
J	Q	-	I	9,601		
E	I	150	B	Broke under head	6560	
E	II	150	B	Broke under head	6295	
E	III	75	B	Broke under head	5820	
E	V	150	I	Broke under head	6508	
J	K	250	B	3,940	c	115,070
J	J	250	B	2,670	c	73,730
J	P	250	B	2,530	c	69,870
E	13	-	B	10,060	7000	278,000
E	11	-	I	10,129	8360	288,000
J	014	-	B	7,740	c	214,000
J	13	Baked only	B	6,460	c	179,000
E	14	150	B	Broke under head	7650	
J	014	250	B	6,410	c	177,100
J	013	250	I	7,106	c	201,400

[a]Charged specimens plated 20 min at 330 mA, baked 30 min at 150°C.
[b]Machine used:
B--Baldwin-Southwark, loading rate 1440 lb/min, stress values normalized to Instron data.
I--Instron, crosshead speed 0.02 cm/min.
[c]Failed at maximum load.

TABLE C-II. Stress-Rupture Tests of Type 4340 Steel
Notch-tensile Specimens

Ident.	H[a] Charge, mA-min	Conditions	Load, lb (Lever Factor 20)	Stress, psi	Hours to Failure
B	-	Control	380	215,400	No 121
B	-	Reloaded	420	238,000	<0.01
A	300	Slight overcharge	260	147,400	<0.01
C	250		220	125,000	0.02
D	250		180	102,000	0.03
E	250		140	79,340	0.03
F	250		100	56,680	53.7
G	250		120	(68,000)[d]	48.2
H	80	Low charge	140	79,340	0.01
L	0	No charge; plate and bake only	160	90,690	No 144
M	250	Aged 6 days after bake	160	90,690	0.07
L[b]	300	No bake; aged 2 days	140	79,340	0.02
N	250	18-hr age before bake	110	62,350	No 123
N	250	Reloaded	150	(85,000)[d]	0.37
B	250	Baked 55 hr at 300°F	380	215,400	No 100
B	250		125	70,850	No 100
B	250	Reloaded	140	79,340	0.03
0 1	250	No poison	140	79,340	No 96
0 1	250	Reloaded	180	102,000	61.6
0 12	250	Irradiated	140	79,340	10.8
0 12	250[c]	Irradiated, baked 360 min	280	158,700	<0.01
12	250[c]	Irradiated, baked 190 min	180	102,000	8.8
11	250	Irradiated	160	90,690	0.03
11	250[c]	Irradiated, baked 300 min	200	113,360	0.03

[a]All charged specimens plated 20 min at 330 mA, baked 30 min at 150°C, unless otherwise stated.
[b]Cadmium plate stripped from L, baked in vacuum, recharged.
[c]No poison in charging acid.
[d]Broke under head.

TABLE C-III. Tensile Tests of Unirradiated Type 212-B Steel

Type	Ident.	H[a] Charge, mA-min	Machine[b]	Load at Yield, lb	Maximum Load, lb	Load at Failure, lb	Maximum Load[c] Original Cross-sectional Area, psi
			Uncharged				
E	-	-	B	1240	2690		76,260
E	-	-	B	1220	2680		75,970
E	III	-	I	1298	2684	1867	76,060
J	-	-	B	2290	3660		103,660
J	L	-	I	2508	3687	2970	104,500
J	K[d]	-	I	3124	3683	3467	104,400
J	Q	-	I	2960	3639	2970	104,100
J	T	-	I		3722		105,480
			Hydrogenated; Charge A (30-min bake)				
E	I	150[e]	B	1380	2670	1800	77,600
E	II	150	B	1410	2680	1800	75,970
E	IV	150	I	1410	2675	2000	75,800
J	I	250[e]	B	2200	3490		101,500
J	II	250[e]	B	2260	3570	3200	103,800
J	M	1250	I	2190	3617	3357	102,500
			Hydrogenated; High Charge (10-min bake)				
E	V	72,000	I		2596		73,570
J	R	60,000	I		3344		94,770
J	S	60,000	I		3190		90,400
J	8	120,000	I	2940	3351	3010	95,000
J	Z	121,000	I	2300	3256		92,270

[a]All J-type specimens cadmium-plated 20 min at 330 mA. E-type specimens have 0.6 area of J-type. Current reduced 0.6 for both charging and plating E-type specimens.

[b]Machine used:

I--Instron, crosshead speed 0.02 cm/min.

B--Baldwin-Southwark, loading rate 1440 lb/min. Stress values normalized to Instron data.

[c]TS for E-type, NTS for J-type.

[d]Specimen previously tested for delayed failure. No break in 100 hr.

[e]Specimen not baked.

TABLE C-IV. Tensile Tests of Irradiated Type 212-B Steel

Ident. (All notched J specimens)	H[a] Charge, mA-min	Machine[b]	Load at Yield, lb	Maximum Load, lb	Load at Failure, lb	Maximum Load[c] Original Cross-sectional Area, psi
		Uncharged				
1	-	B	3300	4540		128,780
2	(baked)	B	3820	4600		129,900
2	-	B	4900	4600	4390	130,050
7	-	I		4787		135,660
5	-	B	4600	4940	4170	140,180
		Hydrogenated; Charge A (30-min bake)				
1	250	B	3540	4360		123,560
2	250	B	4270	4600		129,900
0	250[d]	I	4400	4609	3993	130,600
5	250[d]	I	4400	4710		133,500
		Hydrogenated; High Charge (10-min bake)				
7	124,000	I		4325		122,570
4	60,000[d]	I		4455		126,600

[a]All J-type specimens cadmium-plated 20 min at 330 mA. E-type specimens have 0.6 area of J-type. Current reduced 0.6 for both charging and plating E-type specimens.
[b]Machine used:
I--Instron, crosshead speed 0.02 cm/min.
B--Baldwin-Southwark, loading rate 1440 lb/min. Stress values normalized to Instron data.
[c]TS for E-type, NTS for J-type.
[d]Specimen previously tested for delayed failure. No break in 100 hr.

TABLE C-V. Stress-Rupture Tests of Type 212-B Steel Notch-tensile Specimens (Unirradiated)

Ident.	H[a] Charge, mA-min	Load, lb	Stress, psi	Hours to Failure
	Uncharged			
-	-	200	113,400	<0.01
-	-	190	107,700	<0.01
-	-	180	102,000	No 185.6
-	-	170	96,350	No 191.6
-	-	180	102,000	1.4
H	-	180	102,000	0.6
K	-	175	99,200	No 193
	Hydrogenated; Charge A (30-min bake)			
E	-	170	96,350	No 69
E	250	170	96,350	No 23
A	275	160	90,650	67
A	1250	170	96,350	0.01
B	800	160	90,650	15.6
C	650	140	79,340	No 96
C	650	160	90,650	No 49
C	650	180	102,000	<0.01
D	250	160	90,650	No 113
D	250	180	102,000	0.01
F	250	170	96,350	6.1
G	250	165	93,400	No 232
	Hydrogenated; High Charge (10-min bake)			
8	67,500	140	79,340	No 116
8	117,000	160	90,650	0
8	233,500	155	87,850	0.5

[a]All J-type specimens cadmium-plated 20 min at 330 mA. E-type specimens have 0.6 area of J-type. Current reduced 0.6 for both charging and plating E-type specimens.

TABLE C-VI. Stress-Rupture Tests of Irradiated Type 212-B Steel Notch-tensile Specimens

Ident.	H[a] Charge, mA-min	Load, lb	Stress, psi	Hours to Failure
		Uncharged		
4	-	250	127,550	2.3
4	-	220	124,700	No 111.9
7	-	222	125,830	4.0
		Hydrogenated; Charge A (30-min bake)		
1	250	220	124,700	0.05
0	250	200	113,400	No 96.6
0	250	220	124,700	0.2
0	250	210	119,000	16.2
5	2000	210	119,000	51.7
5	250	210	119,000	
		Hydrogenated; High Charge (10-min bake)		
6	121,500	195	110,530	5.5
6	121,200	192	108,830	2.0
6	120,000	180	102,000	No 113.8
3	120,000	208	117,890	0.12

[a]All J-type specimens cadmium-plated 20 min at 330 mA. E-type specimens have 0.6 area of J-type. Current reduced 0.6 for both charging and plating E-type specimens.

The identification code used during the work is kept for these tables. The number indicates the tier; those with double figures (like 12 :) are Type 4340. Data from the Baldwin tensile machine had to be normalized to make it consistent with that from the Instron. The correction, due to recalibration, is of the order of $2\frac{1}{2}\%$. The loading rates for the two machines are approximately equivalent in the elastic range.

Charging conditions are reported in mA-min, in realization of the limitations discussed in the text. Since the surface area of the shaped E-type specimen is 60% of that for the notched J-type, the current for comparable charging conditions was reduced accordingly for the E specimens.

ACKNOWLEDGMENTS

This work was done partially as a thesis that led to a Ph.D. in Metallurgy from Case Institute of Technology, Cleveland, Ohio. The program was made possible by the policy of Argonne National Laboratory to encourage advanced technical education and cooperation with colleges and universities. Particular thanks are due to Professor A. R. Troiano, Head of the Metallurgy Department of Case, for accepting a graduate student under the special circumstances this program required, and for his continuing interest and advice despite the distance problems involved. At Argonne, the advice and encouragement of T. H. Blewitt has been vital.

The experimental work was accomplished with the cooperation of members of the CP-5 Reactor Staff, the 301 Hot Laboratory crew, the Physics Glass Shop, and members of the Engineering Irradiation Group, in particular, R. J. Fousek, W. C. Kettman, and W. R. Ahrens.

REFERENCES

1. Elsea, A. R., and Fletcher, E. E. (BMI), *Hydrogen-induced, Delayed, Brittle Failures of High-strength Steels*, DMIC Report 196 (Jan. 20, 1964).
2. Fletcher, E. E., and Elsea, A. R., *Hydrogen Movement in Steel, Entry, Diffusion and Elimination*, DMIC Report 219 (June 30, 1965).
3. Smialowski, M., *Hydrogen in Steel*, Pergamon Press (1962).
4. Troiano, A. R., *The Role of Hydrogen and Other Interstitials in the Mechanical Behavior of Metals*, Trans. Am. Soc. Metals *52*, 54 (1960). (1959 E.D. Campbell Memorial Lecture.)
5. Frohmberg, R. P., Barnett, W. J., and Troiano, A. R., *Delayed Failure and Hydrogen Embrittlement in Steel*, Trans. Am. Soc. Metals *47*, 892-923 (1955).
6. Slaughter, Edward R., Fletcher, E. Ellis, Elsea, Arthur R., and Manning, George K., *An Investigation of the Effects of Hydrogen on the Brittle Failure of High-strength Steels*, WADC TR 56-83 (June 1955).
7. Johnson, H. H., Morlet, J. G., and Troiano, A. R., *Hydrogen, Crack Initiation, and Delayed Failure in Steel*, WADC TR 57-262 (May 1957).
8. Barnett, W. J., and Troiano, A. R., *Crack Propagation in the Hydrogen-induced Brittle Fracture of Steel*, WADC TN 55-405 (Aug 1955).
9. Sims, C. E., *Hydrogen Elimination by Aging*, Trans. AIME *188*, 1321 (1950); J. Metals *188*(11), 1321 (Nov 1950).
10. Johnson, H. H., Morlet, J. G., and Troiano, A. R., *Hydrogen, Crack Initiation, and Delayed Failure in Steel*, Trans. Met. Soc. AIME *212*(4), 528-536 (Aug 1958).
11. Steigerwald, E. A., Shaller, F. W., and Troiano, A. R., *Discontinuous Crack Growth in Hydrogenated Steel*, Trans. Met. Soc. AIME *215*, 1048 (Dec 1959).
12. Gray, H. R., and Troiano, A. R., *Hydrogen in Maraging Steel*, Progress Report No. IV, Case Institute of Technology (June 1964).
13. Steigerwald, E. A., Schaller, F. W., and Troiano, A. R., *The Role of Stress in Hydrogen Induced Delayed Failure*, Trans. Met. Soc. AIME *218*, 832-841 (Oct 1960).
14. Simcoe, C. R., Elsea, A. R., and Manning, G. K., *An Investigation of Absorbed Hydrogen in Ultra-high-strength Steel*, WADC TR 56-598, BMI (Nov. 15, 1956).
15. Smialowski, M., *Hydrogen in Steel*, Pergamon Press, pp. 88-89 (1962).
16. Raring, R. H., and Rinebolt, J. A., *Static Fatigue of High-strength Steel*, NRL Memorandum Report 452 (April 1955).
17. Johnson, H. H., Schneider, E. J., and Troiano, A. R., *The Recovery of Embrittled Cadmium-plated Steel*, WADC TC 57-340 (June 1957).
18. McCoy, H. E., Jr., *The Effects of Hydrogen on the High-temperature Flow and Fracture Characteristics of Metals*, ORNL-3600 (1965).

19. Cain, W. M., and Troiano, A. R., *Steel Structure and Hydrogen Embrittlement*, Petroleum Engineer (May 1965).

20. Johnson, R. D., Johnson, H. H., Barnett, W. J., and Troiano, A. R., *Hydrogen Embrittlement and Static Fatigue in High Strength Steel*, WADC TN 55-404 (Aug 1955).

21. Whiteman, M. B., *The Influence of Hydrogen on Metastable FCC Alloys*, Ph.D. thesis, Case Institute of Technology (1965).

22. Nichols, R. W., and Harries, D. R., *Brittle Fracture and Irradiation Effects in Ferritic Pressure Vessel Steels*, ASTM-STP-34, pp. 162-198 (1963).

23. Cibois, E., Lemaire, J., and Weisz, M., *Irradiation Embrittlement and Hardening of Steels and Zircaloy-2 in Pressurized Components*, ASTM-STP-341, pp. 253-274 (1963).

24. Billington, D. S., and Crawford, J. H., *Radiation Damage in Solids*, Princeton University Press, p. 144 (1961).

25. Steele, L. E., and Hawthorne, J. R., *New Information on Neutron Embrittlement and Embrittlement Relief of Reactor Pressure Vessel Steels*, ASTM-STP-380, p. 289, Baltimore (1965).

26. Rossin, A. D., *Comparison of Neutron Embrittlement of Steel in Different Reactor Spectra*, Nuclear Structural Engineering *1*, 76-82 (1965).

27. Rossin, A. D., *Dosimetry for Radiation Damage Studies*, ANL-6826 (March 1964).

28. Balai, N., Sutton, C. R., Wimunc, E. A., and Jones, R. F., *Inspection, Evaluation, and Operation of the EBWR Reactor Vessel*, ANL-7117 (Nov 1965).

29. *Evaluation of YANKEE Vessel Cladding Penetrations*, WCAP-2855, Westinghouse Atomic Power Division, Pittsburgh (Oct. 15, 1965).

30. Broomfield, G. H., *Hydrogen Effects in an Irradiated 1% Cr, 1/2% Mo PWR Pressure Vessel Steel*, AERE-R-4705 (Sept 1964).

31. Claudson, T. T., *Fabrication History of Alloys used in the Irradiation Effects on Reactor Structural Materials Program*, BNWL-CC-236, Section IIIA (Oct 1965).

32. Rossin, A. D., *Significance of Neutron Spectrum on Radiation Effects Studies*, ASTM-STP-341, pp. 115-132, Baltimore (1963).

33. Johnson, H. H., Johnson, R. D., Frohmberg, R. P., and Troiano, A. R., *Static Fatigue in Twelve Heats of 4340 Steel Embrittled with Hydrogen*, WADC TN 55-306 (Aug 1955).

34. Hobson, J. D., and Sykes, C., *Effect of Hydrogen on the Properties of Low Alloy Steels*, J. Iron Steel Inst. *169*, 209-220 (1951).

35. Harries, D. R., and Broomfield, G. H., *Hydrogen Embrittlement of Steel Pressure Vessels in Pressurized Water Reactor Systems*, J. Nucl. Materials *9*(3), 327 (1963).